SUPPLEMENTAL INFORMATION

**SpoVAF and FigP assemble into oligomeric ion channels that enhance spore germination**

Yongqiang Gao, Jeremy D. Amon, Anna P. Brogan, Lior Artzi, Fernando H. Ramírez-Guadiana, Joshua C. Cofsky, Andrew C. Kruse, David Z. Rudner

**This PDF file includes:**

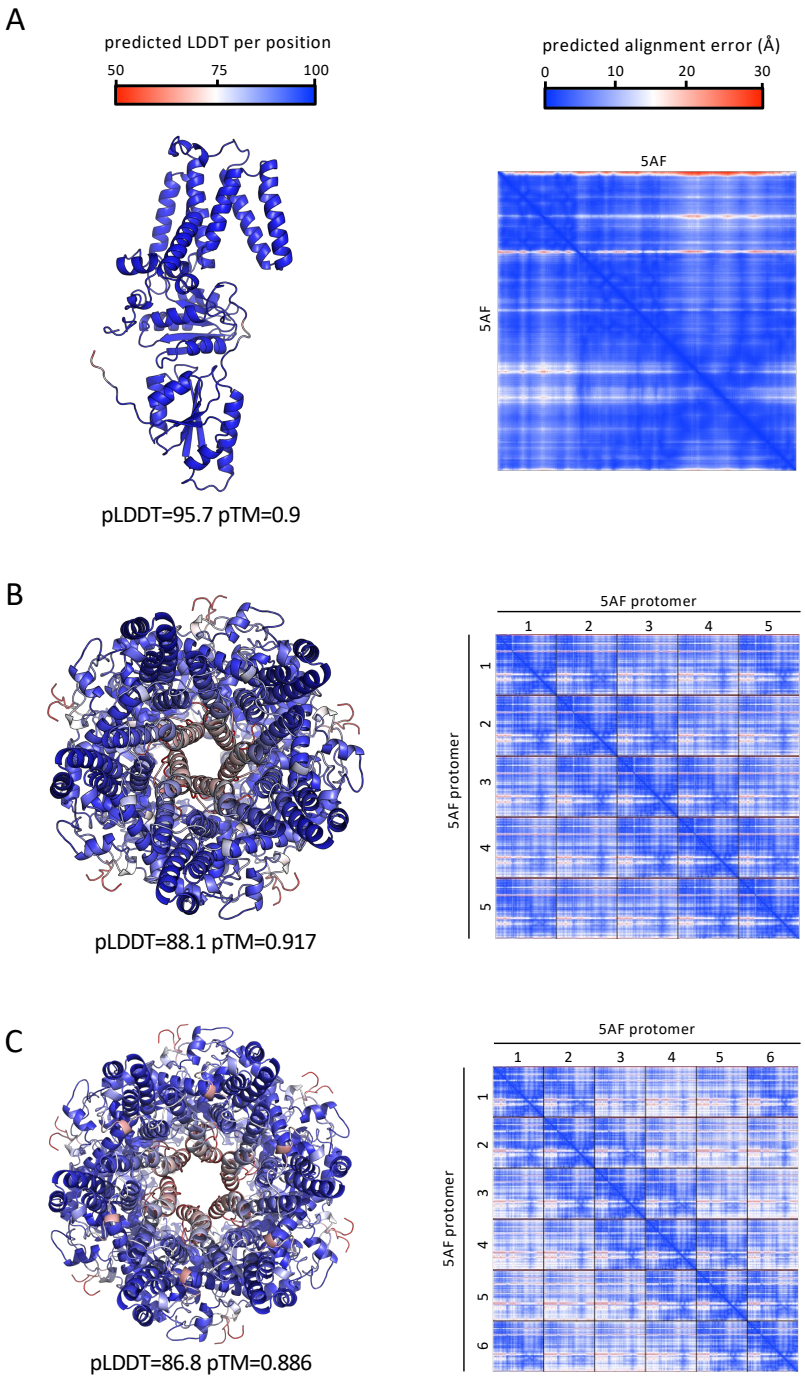


**Figure S1. Predicted local distance difference tests and alignment error for the AlphaFold-predicted 5AF monomer and oligomers. (A)** Predicted local distance difference tests (pLDDT) per position mapped onto the 5AF model (left). Higher pLDDT (blue) corresponds to a more confident prediction. Predicted alignment error in Å of all residues against all residues for the top-ranked 5AF model (right). Low error (blue) corresponds to well-defined relative domain positions. **(B)** Predicted local distance difference tests (pLDDT) per position mapped onto the 5AF pentamer model (left); predicted alignment error in Å of all residues against all residues for the top-ranked model (right). (**C**) Predicted local distance difference tests (pLDDT) per position mapped onto 5AF hexamer (left); predicted alignment error in Å of all residues against all residues for the top-ranked model (right). The per-residue accuracy of the structures (pLDDT) and the estimate of the template modeling scores (pTM) for each model are shown below the predicted structures on the left.

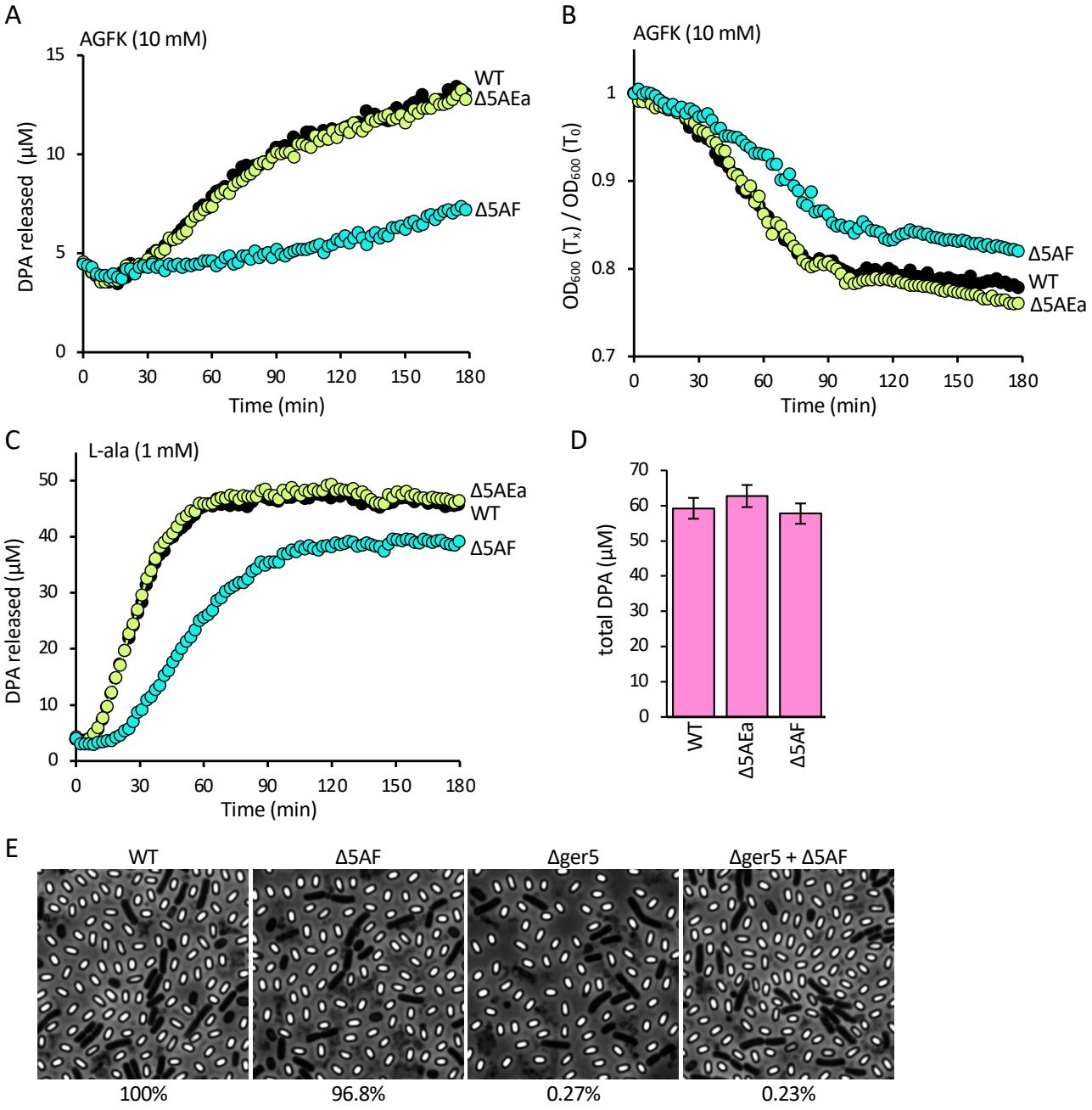


**Figure S2. 5AF enhances germination induced by different nutrients. (A)** Purified *B. subtilis* spores from the indicated strains were incubated with 10 mM each of asparagine, glucose, fructose, and $K^+$ (AGFK) and DPA release was monitored over time. Spores lacking 5FA were delayed in DPA release, while spores lacking 5AEa behaved similarly to wild-type. **(B)** Germination of the same spores as in (A) was assayed using the loss of optical density as the spores transitioned from phase-bright to phase-dark. **(C)** The same spores as in (A) were analyzed for DPA release using 1 mM L-alanine. **(D)** Total DPA present in the purified spores used in the experiments shown in A-C. **(E)** Representative phase-contrast images of 30-hour sporulating cultures of the indicated strains. The total heat-resistant CFU on LB agar plates of each culture relative to wild-type is indicated below the images. The last two strains lack all 5 *gerA* family loci and are labeled Δger5. The receptor-less spores are defective in germination in the presence of nutrient-rich LB.

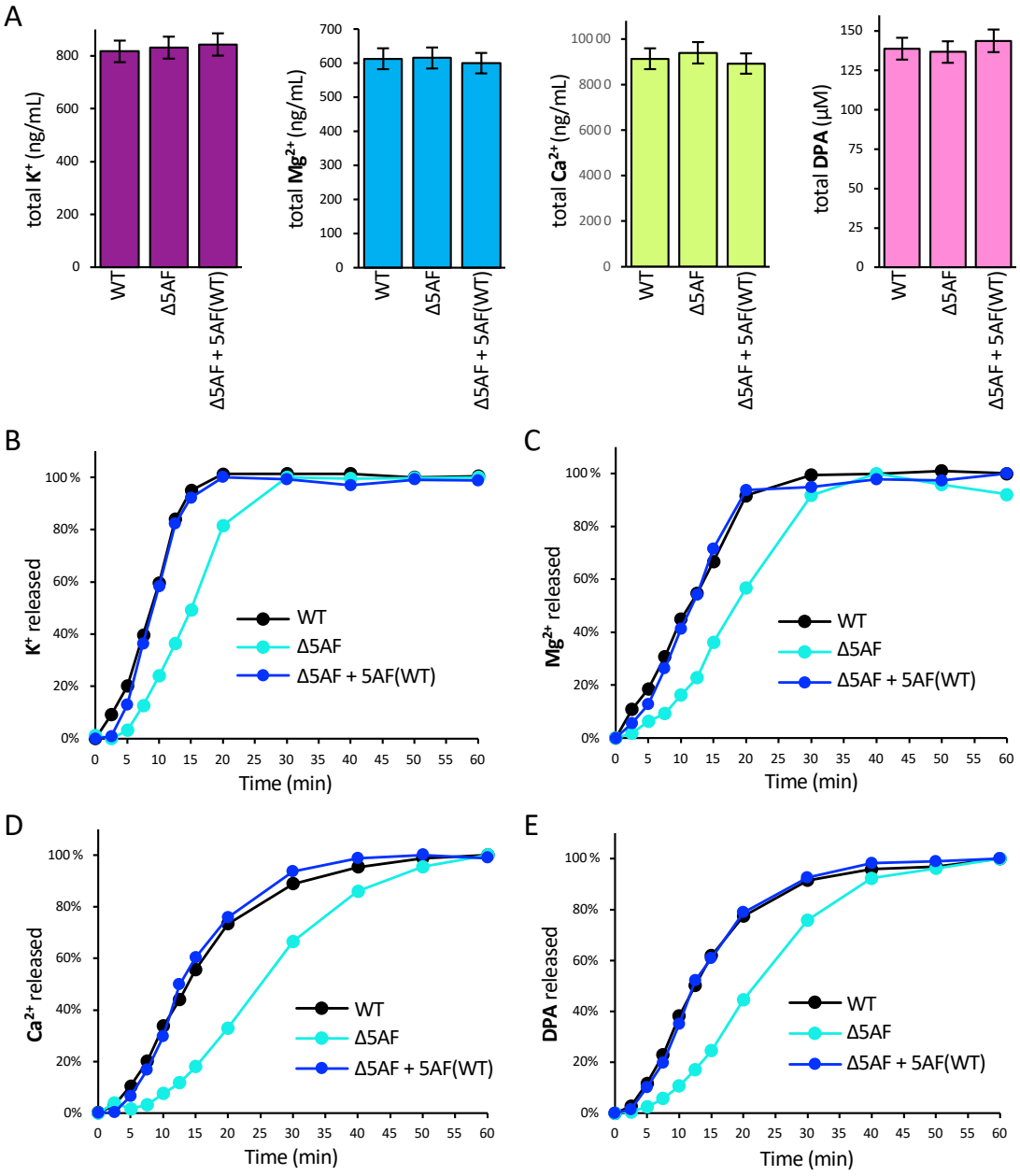


**Figure S3A. Spores lacking 5AF are delayed in $K^+$, $Mg^{2+}$, and $Ca^{2+}$/DPA release. (A)** Total $K^+$, $Mg^{2+}$, $Ca^{2+}$, and DPA in purified spores from the indicated strains determined by inductively coupled mass spectrometry (ICP-MS) or fluorescence with $TbCl_3$. All three strains have similar levels of these molecules. **(B-E)** Analysis of spore exudates after incubation with 10 mM L-alanine for the indicated times. $K^+$, $Mg^{2+}$, and $Ca^{2+}$ were analyzed by ICP-MS and DPA was measured using fluorescence in the presence of $TbCl_3$. The percentage release at each time point, relative to the amount released by WT spores at 60 min, is shown. Spores lacking 5AF were delayed in $K^+$ release **(B)**; in $Mg^{2+}$ release **(C)**; in $Ca^{2+}$ release **(D)**; and in DPA release **(E)**. In all cases, expression of 5AF *in trans* suppressed the defect.

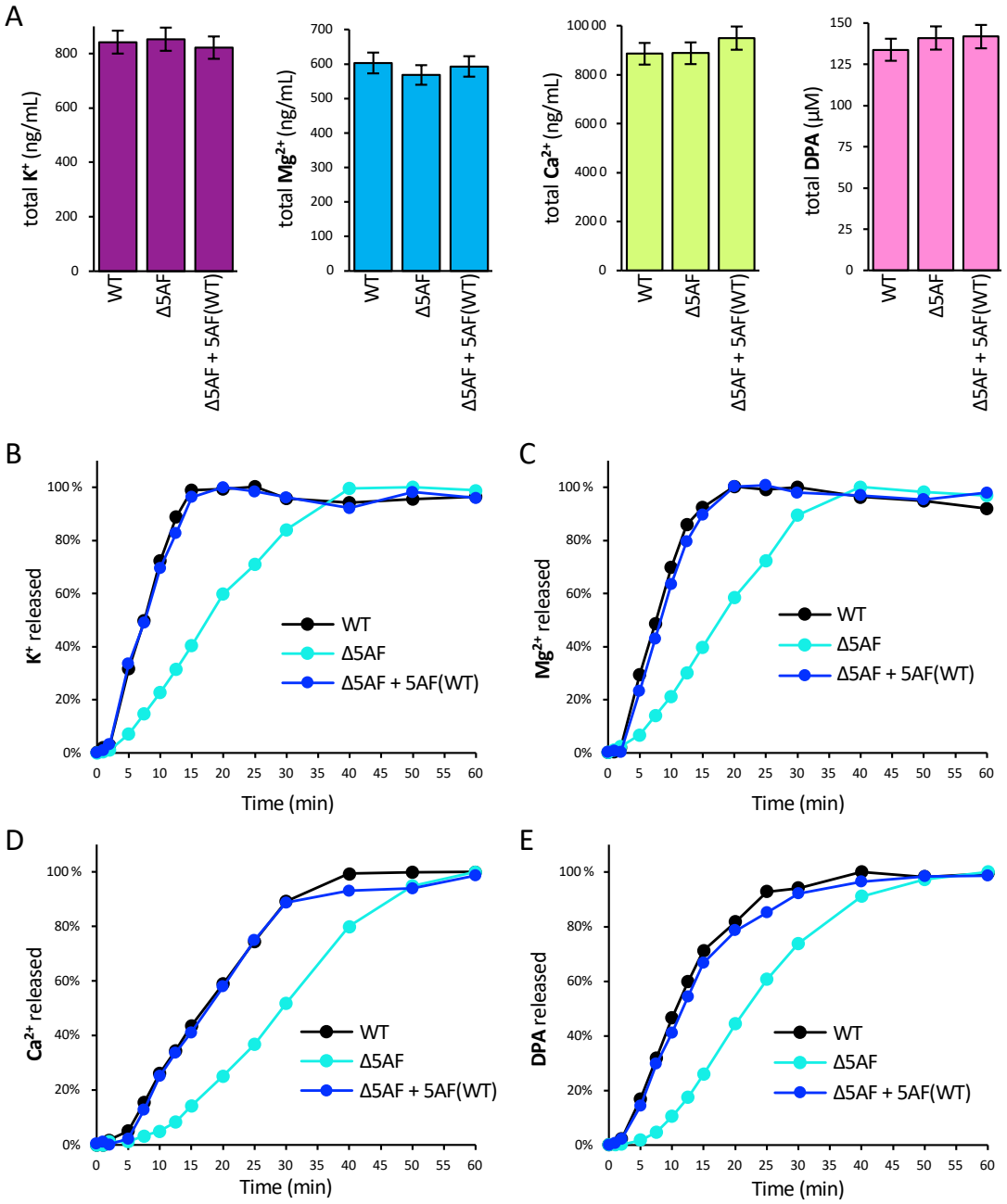


**Figure S3B. Spores lacking 5AF are delayed in $K^+$, $Mg^{2+}$, and $Ca^{2+}$/DPA release.** This figure documents biological replicates of the data presented in Figure S3A. **(A)** Total $K^+$, $Mg^{2+}$, $Ca^{2+}$, and DPA in purified spores from the indicated strains determined by inductively coupled mass spectrometry (ICP-MS) or fluorescence with $TbCl_3$. All three strains have similar levels of these molecules. **(B-E)** Analysis of spore exudates after incubation with 10 mM L-alanine for the indicated times. $K^+$, $Mg^{2+}$, and $Ca^{2+}$ were analyzed by ICP-MS and DPA was measured using fluorescence in the presence of $TbCl_3$. The percentage release at each time point, relative to the amount released by WT spores at 60 min, is shown. Spores lacking 5AF were delayed in $K^+$ release **(B)**; in $Mg^{2+}$ release **(C)**; in $Ca^{2+}$ release **(D)**; and in DPA release **(E)**. In all cases, expression of 5AF *in trans* suppressed the defect.

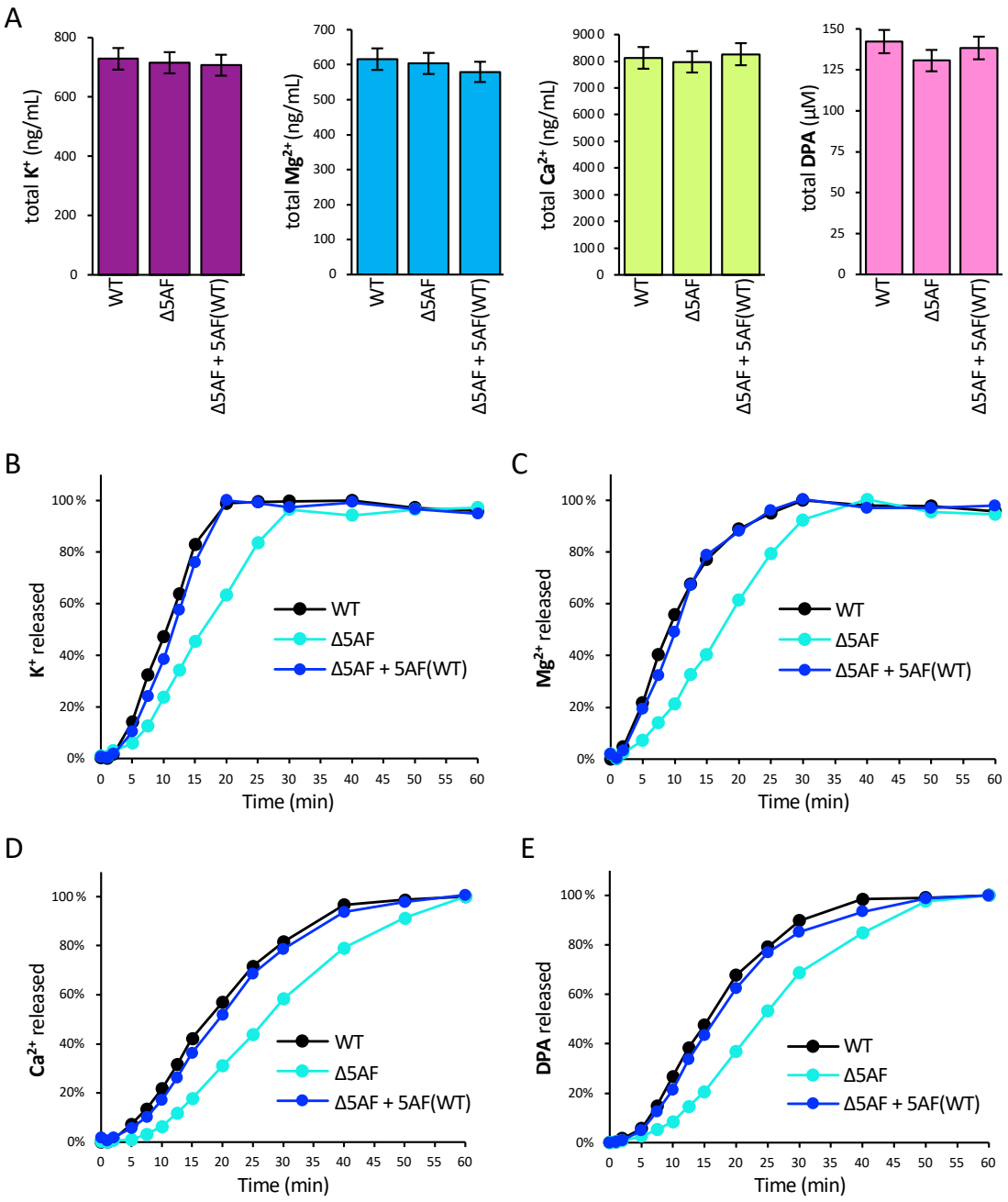


**Figure S3C. Spores lacking 5AF are delayed in $K^+$, $Mg^{2+}$, and $Ca^{2+}$/DPA release.** This figure documents biological replicates of the data presented in Figure S3A. **(A)** Total $K^+$, $Mg^{2+}$, $Ca^{2+}$, and DPA in purified spores from the indicated strains determined by inductively coupled mass spectrometry (ICP-MS) or fluorescence with $TbCl_3$. All three strains have similar levels of these molecules. **(B-E)** Analysis of spore exudates after incubation with 10 mM L-alanine for the indicated times. $K^+$, $Mg^{2+}$, and $Ca^{2+}$ were analyzed by ICP-MS and DPA was measured using fluorescence in the presence of $TbCl_3$. The percentage release at each time point, relative to the amount released by WT spores at 60 min, is shown. Spores lacking 5AF were delayed in $K^+$ release **(B)**; in $Mg^{2+}$ release **(C)**; in $Ca^{2+}$ release **(D)**; and in DPA release **(E)**. In all cases, expression of 5AF *in trans* suppressed the defect.

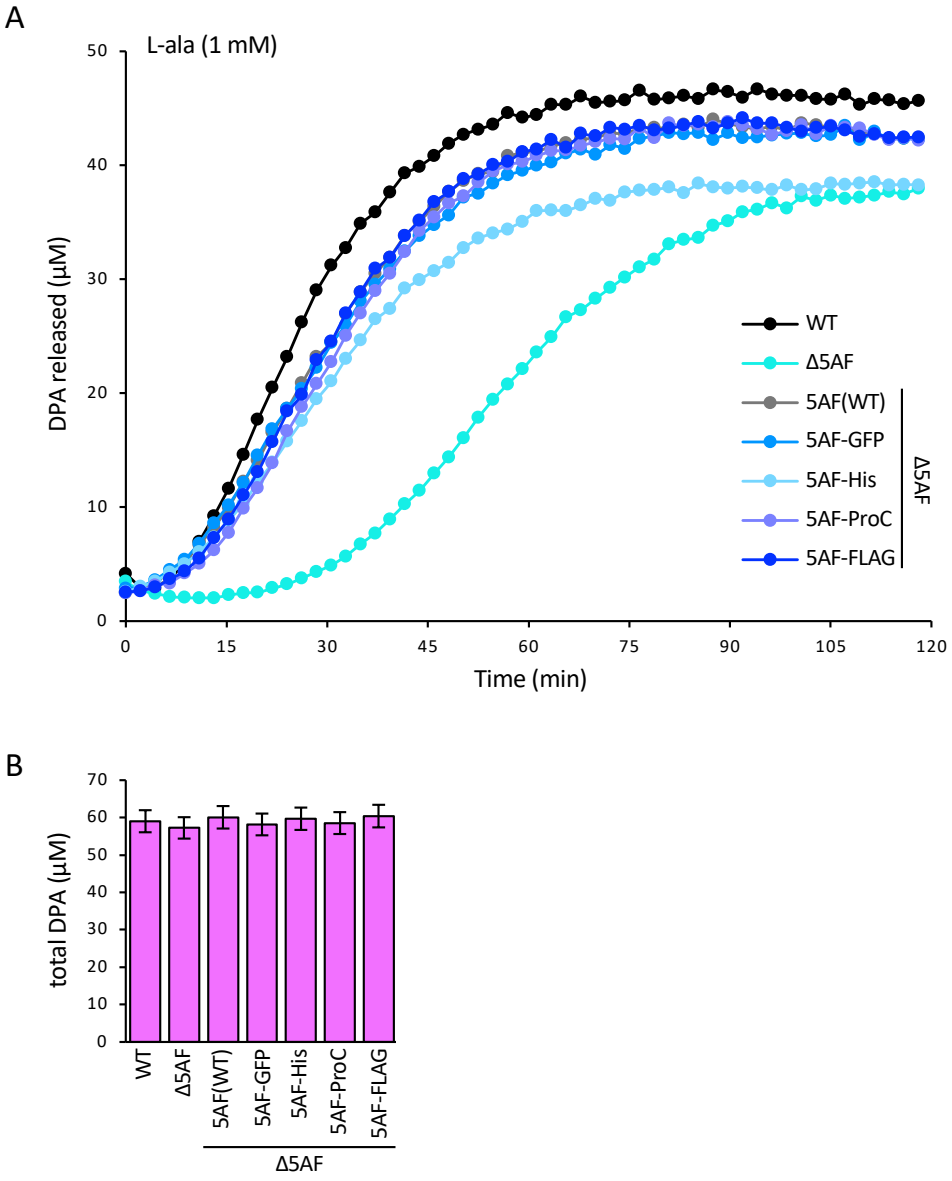


**Figure S4. 5AF fusions are functional. (A)** Purified *B. subtilis* spores from the indicated strains were incubated with 1 mM L-alanine and DPA release was monitored over time. Spores lacking 5FA were delayed in DPA release, while those in which 5AF or the indicated 5AF fusions were expressed *in trans* behaved similarly to wild-type. **(B)** Total DPA present in the purified spores used in the experiment shown in A.

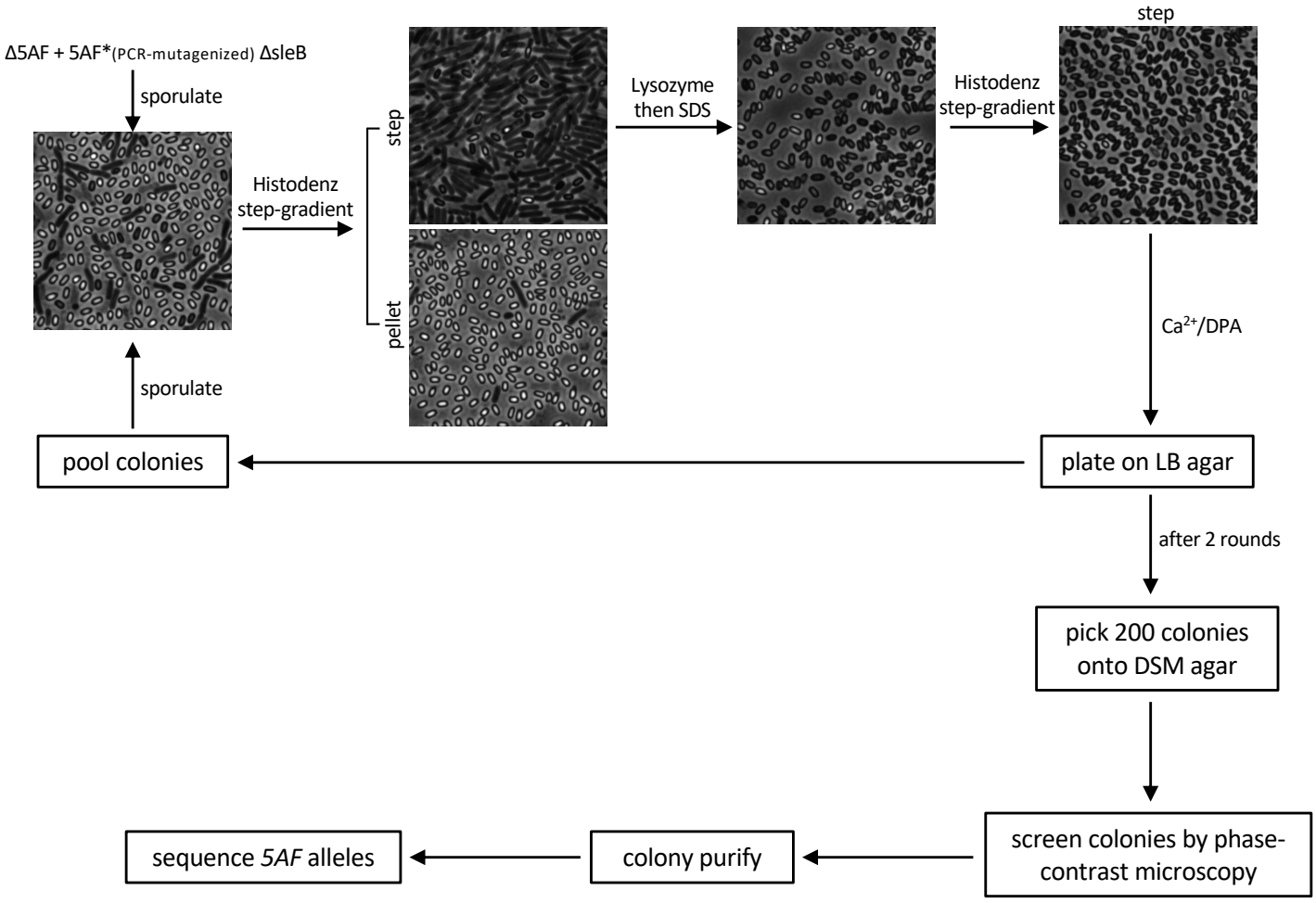


**Figure S5. Flow diagram depicting the screen for constitutively active 5AF mutants that initiate premature germination.** The *5AF* gene was PCR-mutagenized using error prone PCR and transformed into a Δ*5AF* Δ*sleB* mutant. The transformants were pooled and sporulated. The dormant phase-bright spores were separated from vegetative cells and spores that initiated germination on a Histodenz step-gradient. The material in the step was collected and treated with lysozyme followed by SDS to lyse the vegetative cells. Because the phase-grey/dark spores lack SleB they maintain their cortex peptidoglycan and coat and resist lysozyme-SDS treatment. The material was further purified on a second Histodenz step-gradient. The phase-grey/dark spores were collected and incubated with $Ca^{2+}$/DPA to activate CwlJ-dependent degradation of the cortex and plated on LB agar. The colonies were pooled, and a second round of enrichment was performed. After two rounds of enrichment, the purified phase-grey/dark spores were plated on sporulation (DSM) agar. After 96 hours at 37 ˚C, individual colonies were screened by phase-contrast microscopy. Colonies with a high percentage of phase-grey/dark spores were colony-purified. The *5AF* gene was PCR amplified from these strains and Sanger sequenced.

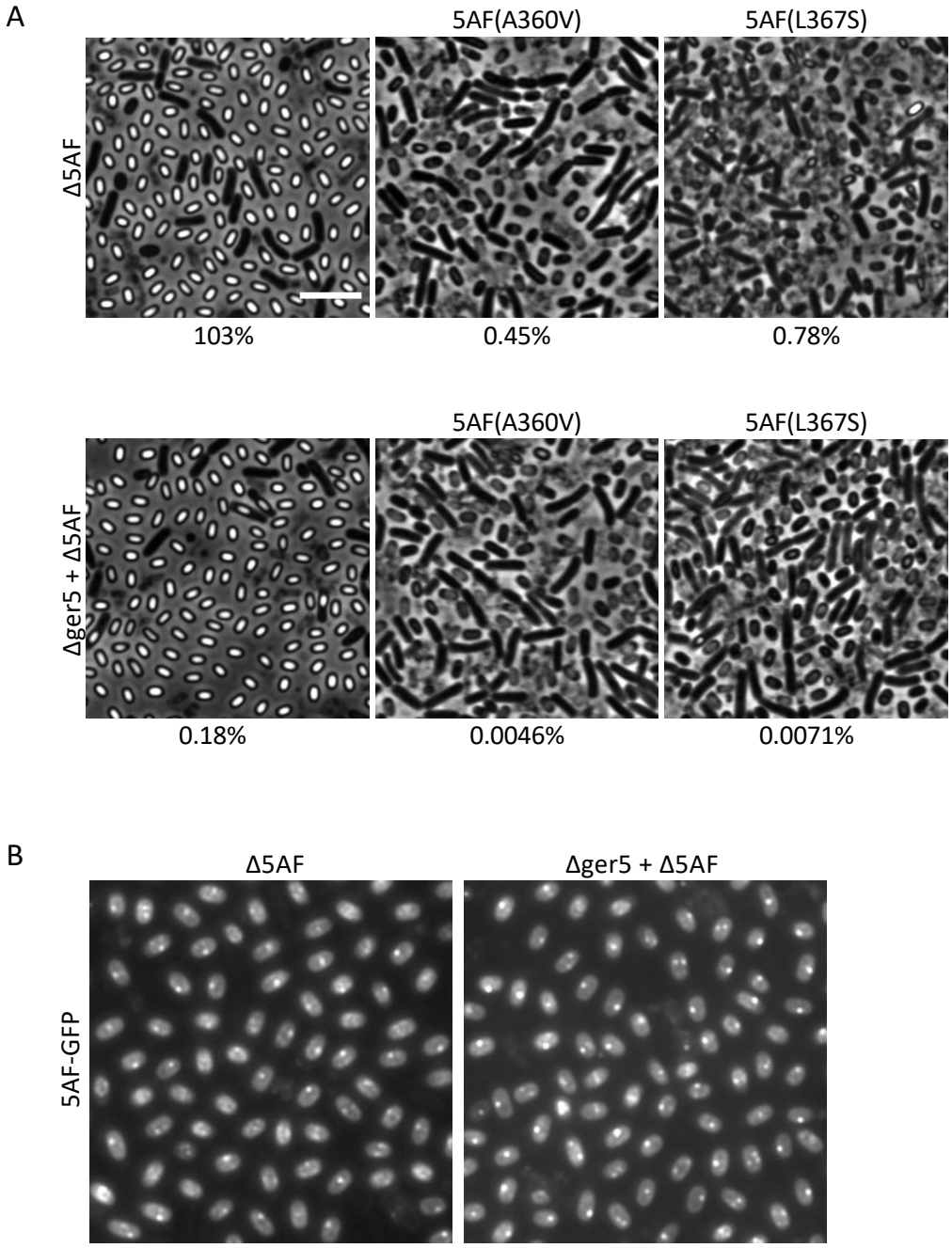


**Figure S6. Constitutively active 5AF mutants cause premature germination in the absence of the GerA family receptors. (A)** Representative phase-contrast images of the indicated strains after 30 hours of sporulation. The constitutively active 5AF mutants cause premature germination in the presence and absence of the five GerA family receptor operons (Δger5). Heat resistant CFU relative to wild-type are shown below the images. All six strains are SleB+. **(B)** Representative fluorescence images of 5AF-GFP in dormant spores of the indicated strains. 5AF-GFP localizes in germinosome foci in the presence and absence of the GerA family receptors (Δger5).

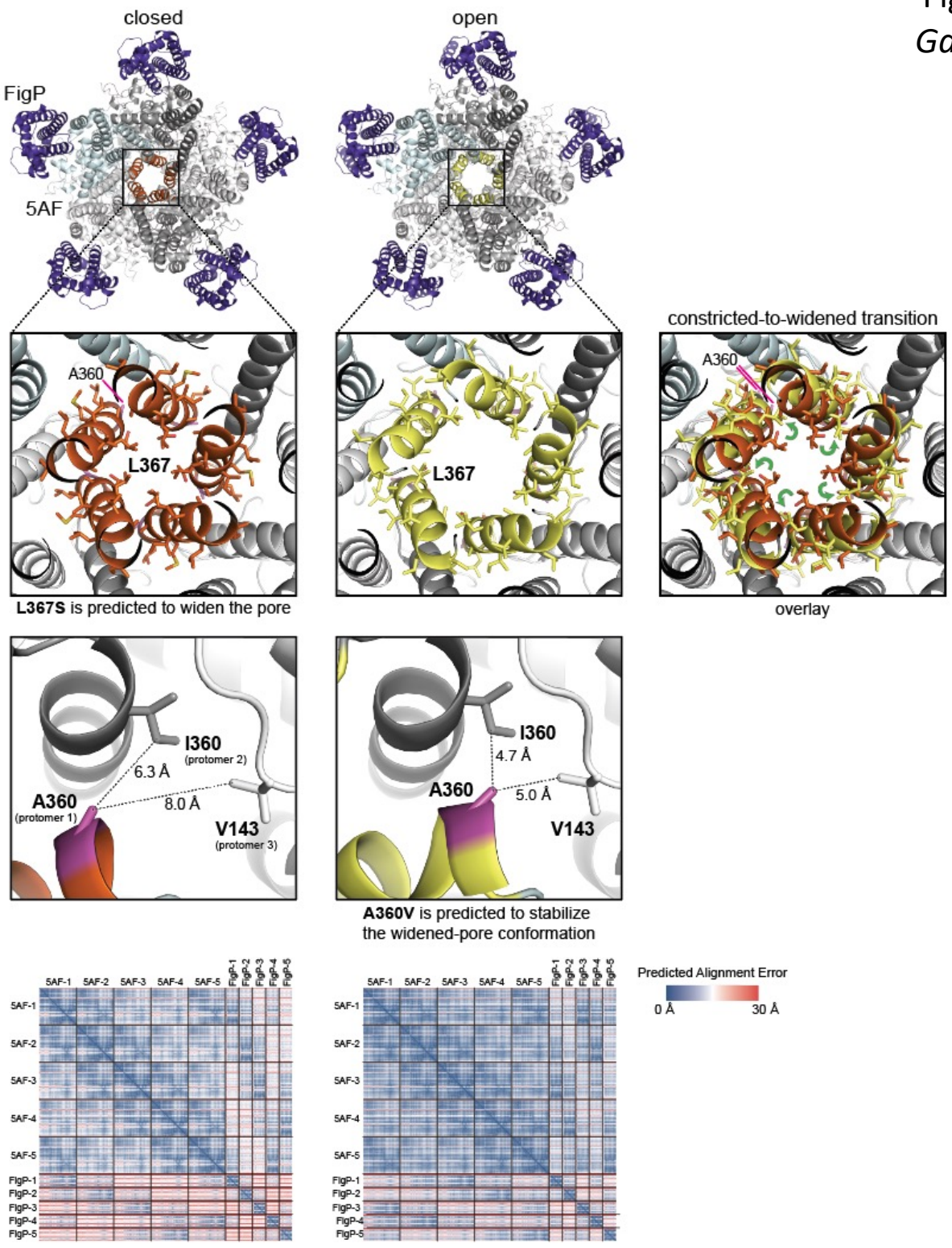


**Figure S7. Two AlphaFold-predicted conformations of the 5AF/FigP pentamer can explain the constitutive activity of 5AF mutants.** In the closed conformation (left), 5AF's pore-forming helices (orange) are oriented such that L367 points into the lumen, forming a constriction in the pore. In open conformation (right), these same helices (yellow) have rotated (green arrows), widening the pore. The L367S substitution is predicted to cause ion leakage, either by removing the bulk of the pore-occluding sidechains or by abolishing the hydrophobic interactions between adjacent L367 sidechains that appear to stabilize the pore constriction. At the base of the pore-forming helix, A360 (pink) closely approaches I355 and V143 from two adjacent protomers. The A360V substitution is predicted to strengthen the hydrophobic interactions between the three sidechains in this region, stabilizing the widened-pore conformation and causing ion leakage. Predicted alignment error plots. Conformation 1 was predicted by AlphaFold model 5 (rank 5). Conformation 2 was predicted by AlphaFold model 4 (rank 1). The structures predicted by AlphaFold models 1 (rank 2), 2 (rank 4), and 3 (rank 3) all resembled Conformation 2.

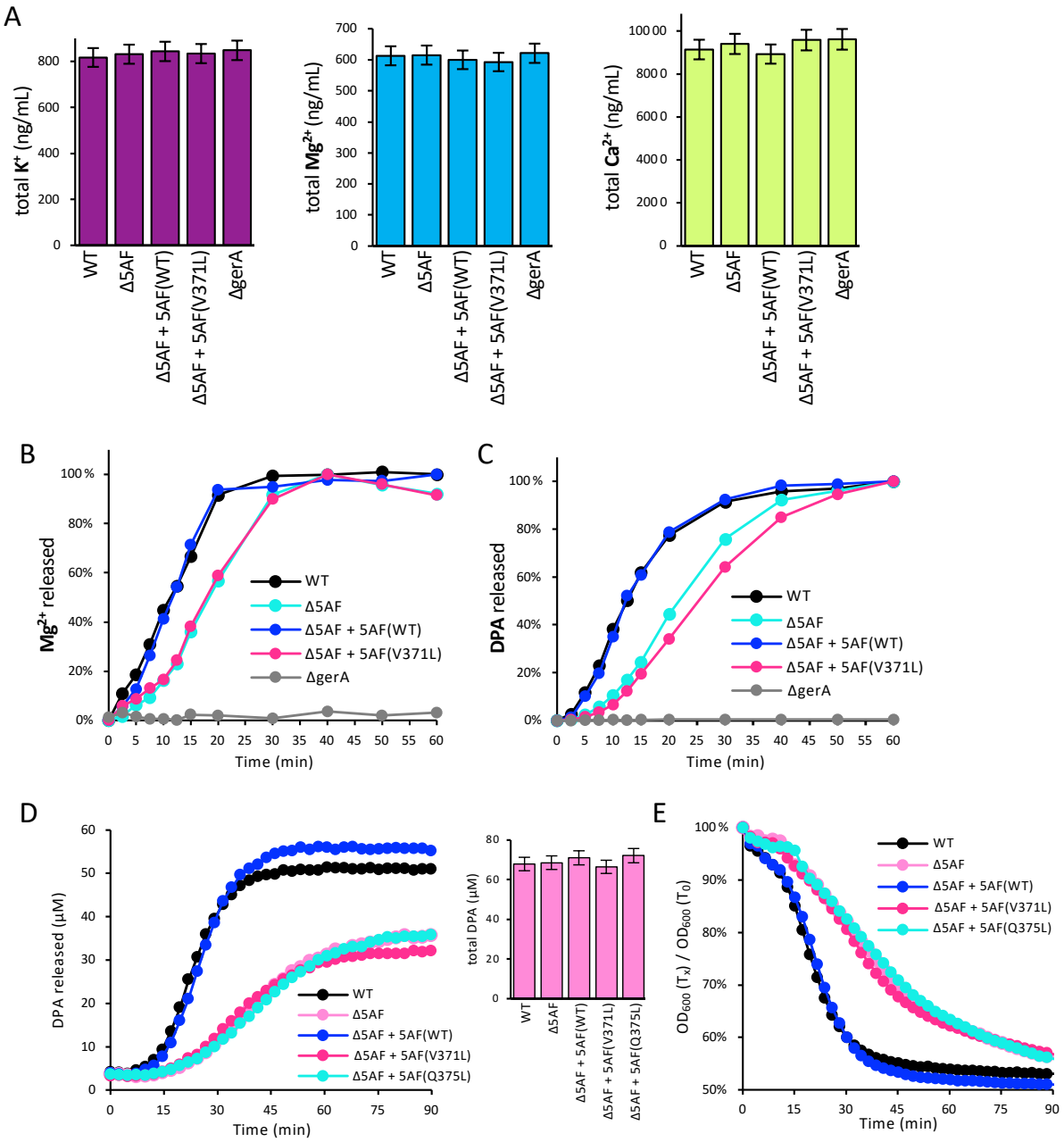


**Figure S8. Spores with the channel narrowing 5AF(V371L) mutant are delayed in germination. (A)** Total $K^+$, $Mg^{2+}$, and $Ca^{2+}$ in purified spores of the indicated strains were determined by inductively coupled mass spectrometry (ICP-MS). All five strains have similar levels of these ions. **(B-C)** Analysis of spore exudates at the indicated times after incubation with 10 mM L-alanine. **(B)** $Mg^{2+}$ was analyzed by ICP-MS. **(C)** DPA was determined using fluorescence in the presence of $TbCl_3$. The percentage release at each time point, relative to the amount released by WT spores at 60 min, is shown. **(D)** The same spores as in (B) and (C) were analyzed for DPA release over time in a plate reader. Total DPA is shown to the right of graph. **(E)** The percentage drop in OD600 was analyzed from the same spores after L-alanine addition in a plate reader. The two channel-narrowing mutants 5AF(V371L) and 5AF(Q375L) phenocopy Δ5AF.

Figure S9
*Gao et al.*

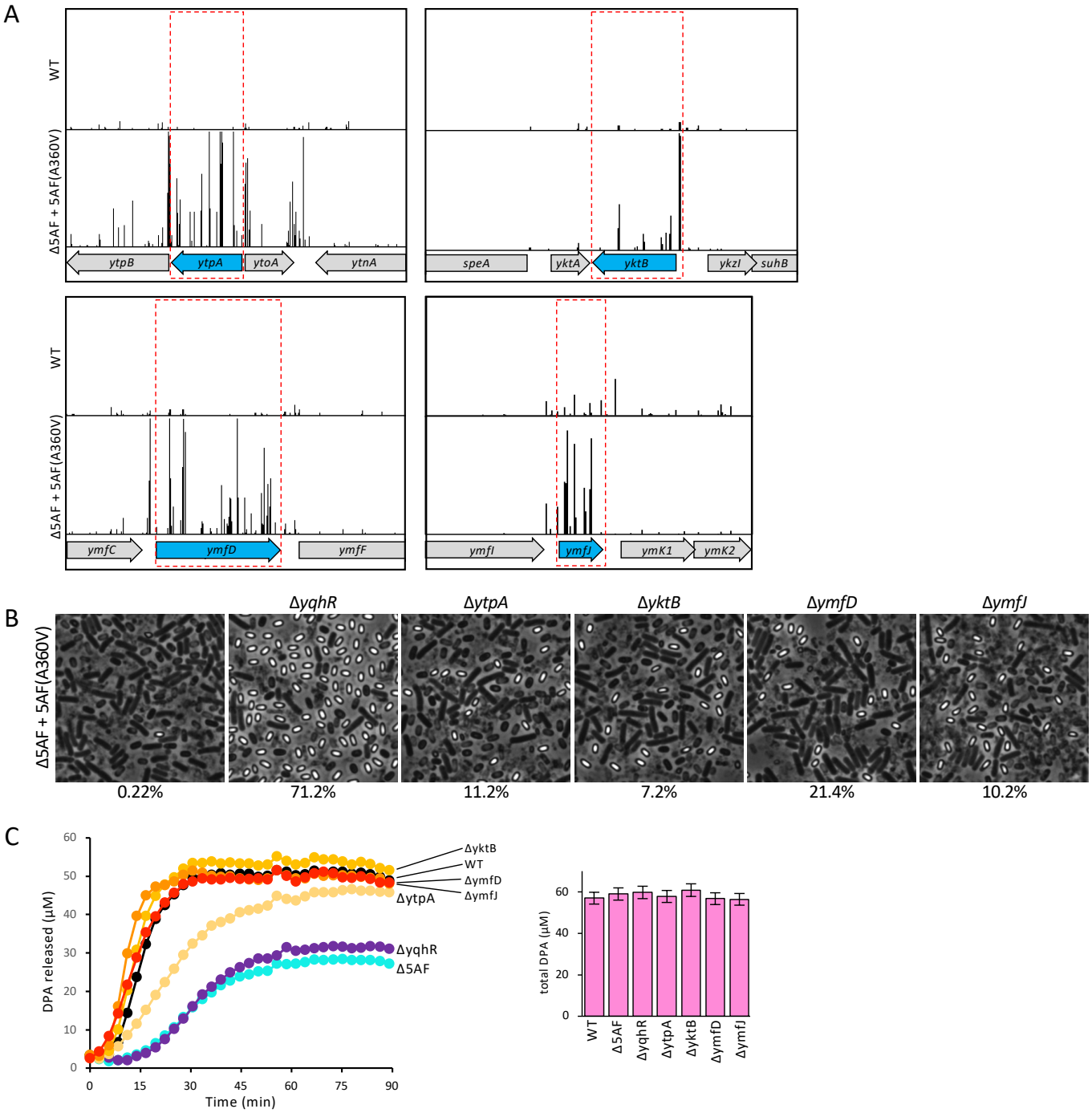


**Figure S9. Identification and initial characterization of the hits in the 5AF(A360V) suppressor screen. (A)** Transposon (Tn) insertion profiles from four genomic regions are shown. Each line represents a Tn insertion site; its height reflects the abundance in the output libraries. The maximum number of reads was set to 10,000 for the regions with *ytpA*, *yktB*, *ymfD* and 2,000 for the region with *ymfJ*. Tn insertions in all four genes were overrepresented in the 5AF(A360V) library compared to WT. **(B)** Representative phase contrast images of sporulated cultures of strains harboring in-frame deletions of the indicated genes. All hits in the screen partially suppress the premature germination phenotype of 5AF(A360V). The percentage of heat-resistance spores compared to wild-type are shown below the images. **(C)** Purified spores from the indicated strains were mixed with 1 mM L-alanine and DPA release was monitored over 90 minutes. All strains lacked 5AF(A360V) and, with the exception of Δ5AF, contained a wild-type copy of 5AF. Total DPA in the purified spores is shown to the right.

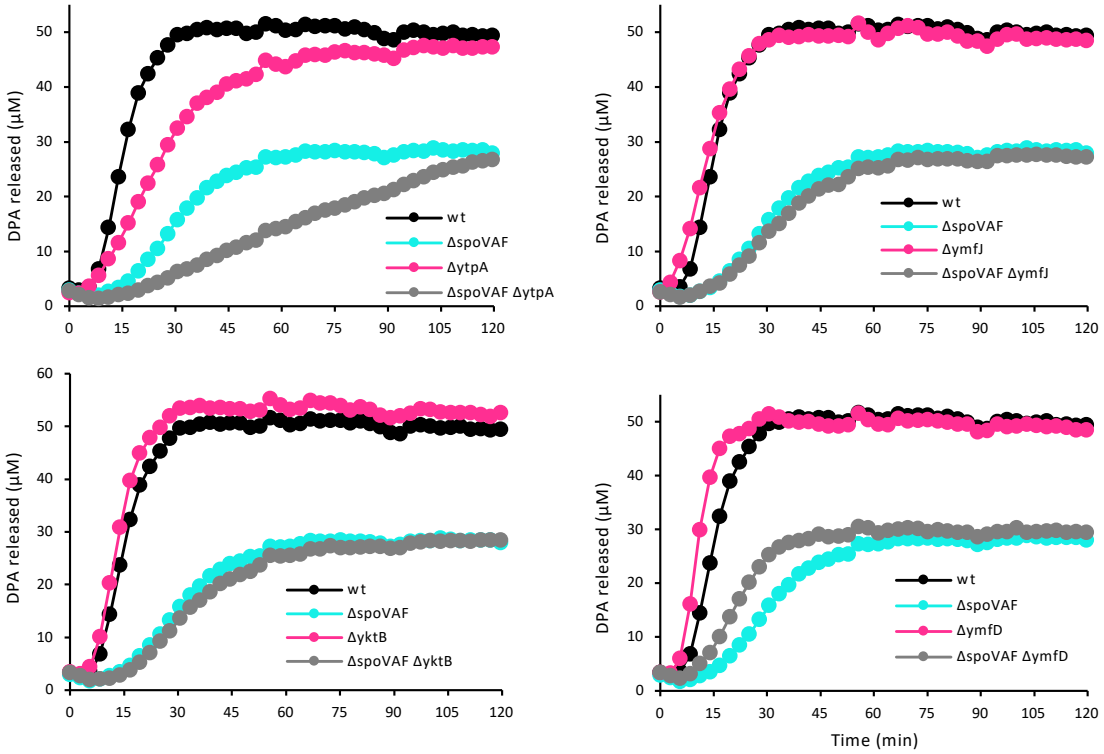


**Figure S10. Double mutant analysis of the 5AF(V360A) suppressors.** Purified spores of the indicated strains were mixed with 1 mM L-alanine and DPA release was monitored over 90 minutes. The Δ*5AF* Δ*ytpA* mutant was more impaired in germination than the single mutants, while the other double mutants resembled the Δ*5AF* single mutant.

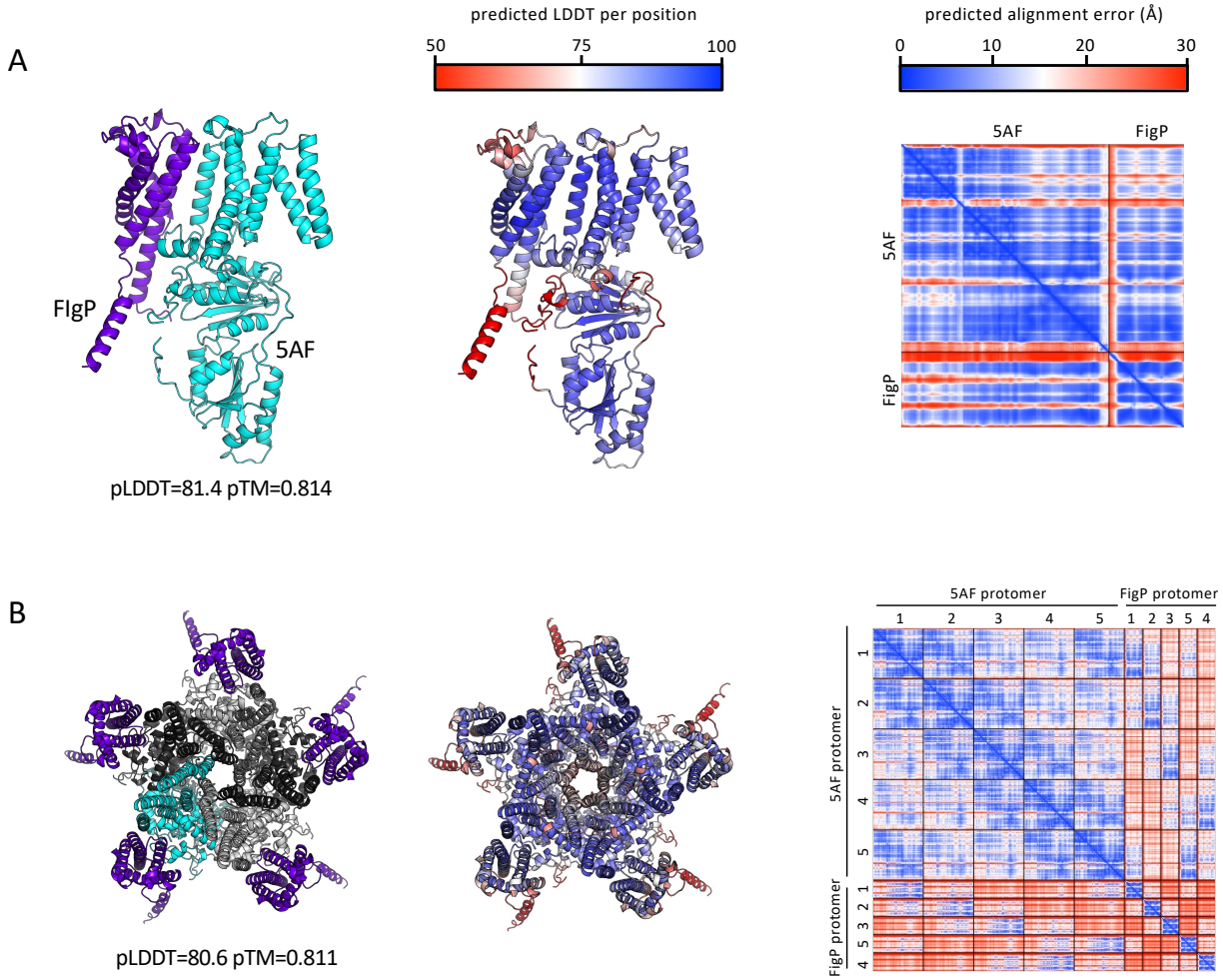


**Figure S11. Predicted local distance difference tests and alignment errors for the AlphaFold-predicted 5AF/FigP dimer and the 5AF/FigP pentamer of dimers. (A)** Model of 5AF/FigP dimer (left). Predicted local distance difference tests (pLDDT) per position mapped onto the 5AF/FigP model (middle). Higher pLDDT (blue) corresponds to a more confident prediction. Predicted alignment error in Å of all residues against all residues for the top-ranked 5AF model (right). Low error (blue) corresponds to well-defined relative domain positions. **(B)** Model of 5AF/FigP pentamer of dimers (left). Predicted local distance difference tests (pLDDT) per position mapped onto the 5AF/FigP pentamer of dimers model (left); predicted alignment error in Å of all residues against all residues for the top-ranked model (right). The per-residue accuracy of the structure (pLDDT) and the estimate of the template modeling score (pTM) for each model is shown below the predicted structures on the left.

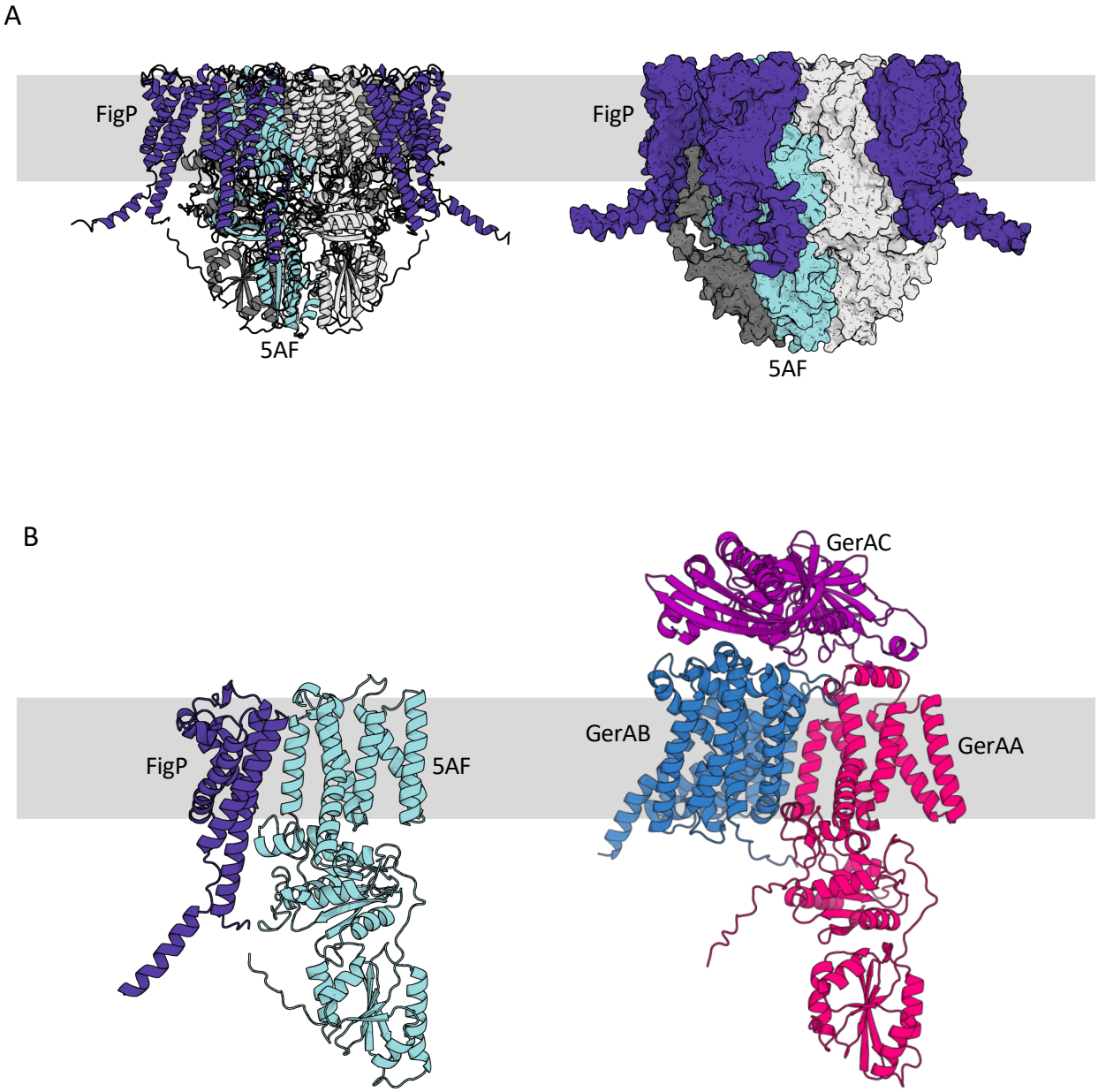


**Figure S12. AlphaFold-predicted model of 5AF and FigP pentamer of dimers as viewed in the membrane. (A)** AlphaFold2-multimer model of the 5AF/FigP pentamer of dimers. 5AF protomers are shown in cyan and light/dark grey. FigP protomers are in purple. **(B)** Comparison of FigP/5AF interaction interface with GerAB/GerAA interaction interface.

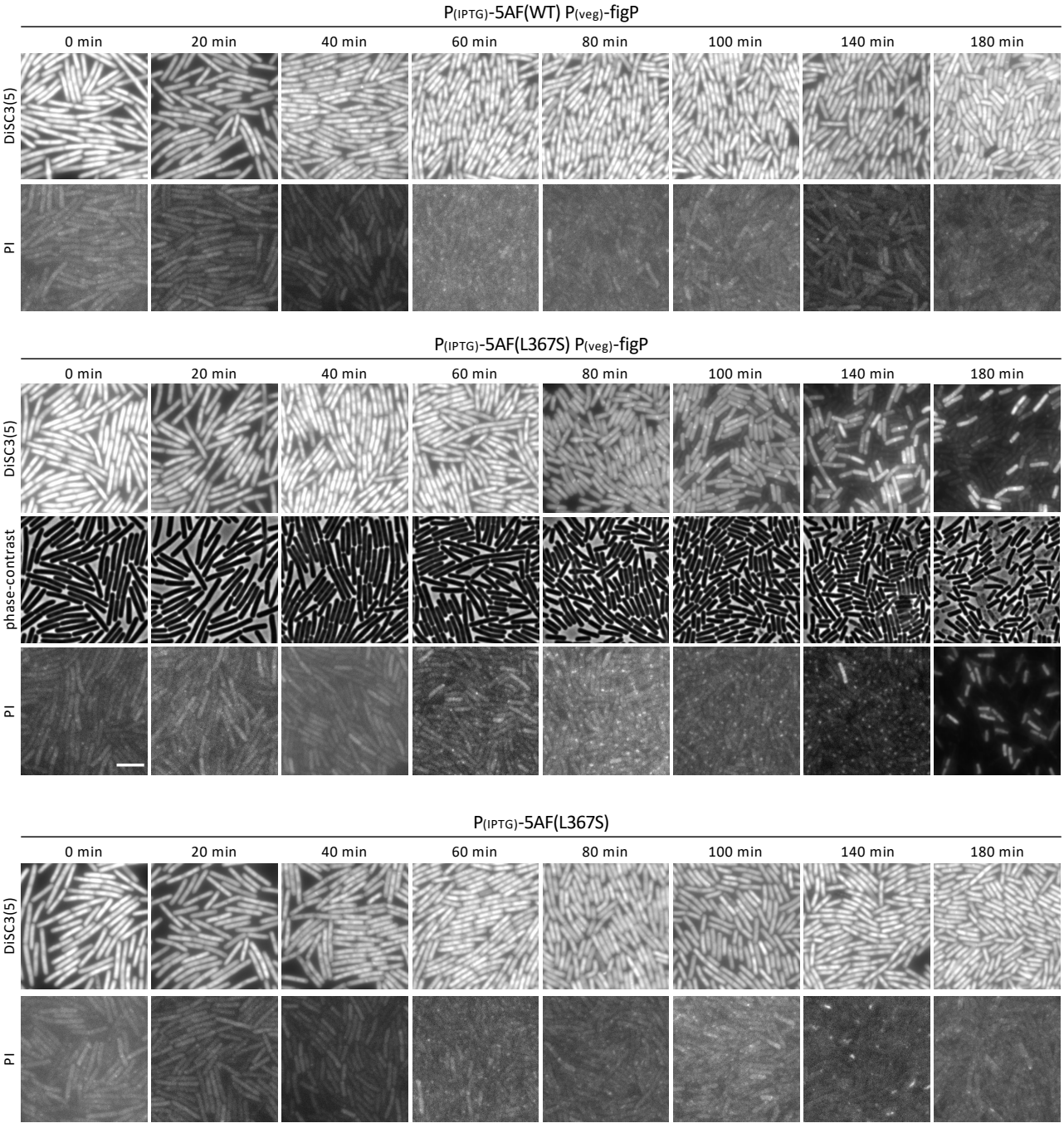


**Figure S13. The 5AF/FigP complex behaves like an ion channel when expressed in vegetatively growing cells.** Representative fluorescence images of exponentially growing cultures of the indicated strains. Time (in min) after IPTG addition (50 μM final) is indicated above each set of images. The upper panels show fluorescence of the potentiometric dye $DiSC_3(5)$; the lower panels show propidium iodide (PI) staining. The two fields are from the same culture and timepoint but were stained and imaged separately. Phase-contrast images are shown for the same fields as the $DiSC_3(5)$ fluorescence images to monitor cell lysis. The loss of membrane potential in cells expressing 5AF(L367S) and FigP occurs prior to loss of membrane integrity and cell lysis. Scale bar, 5 μm.

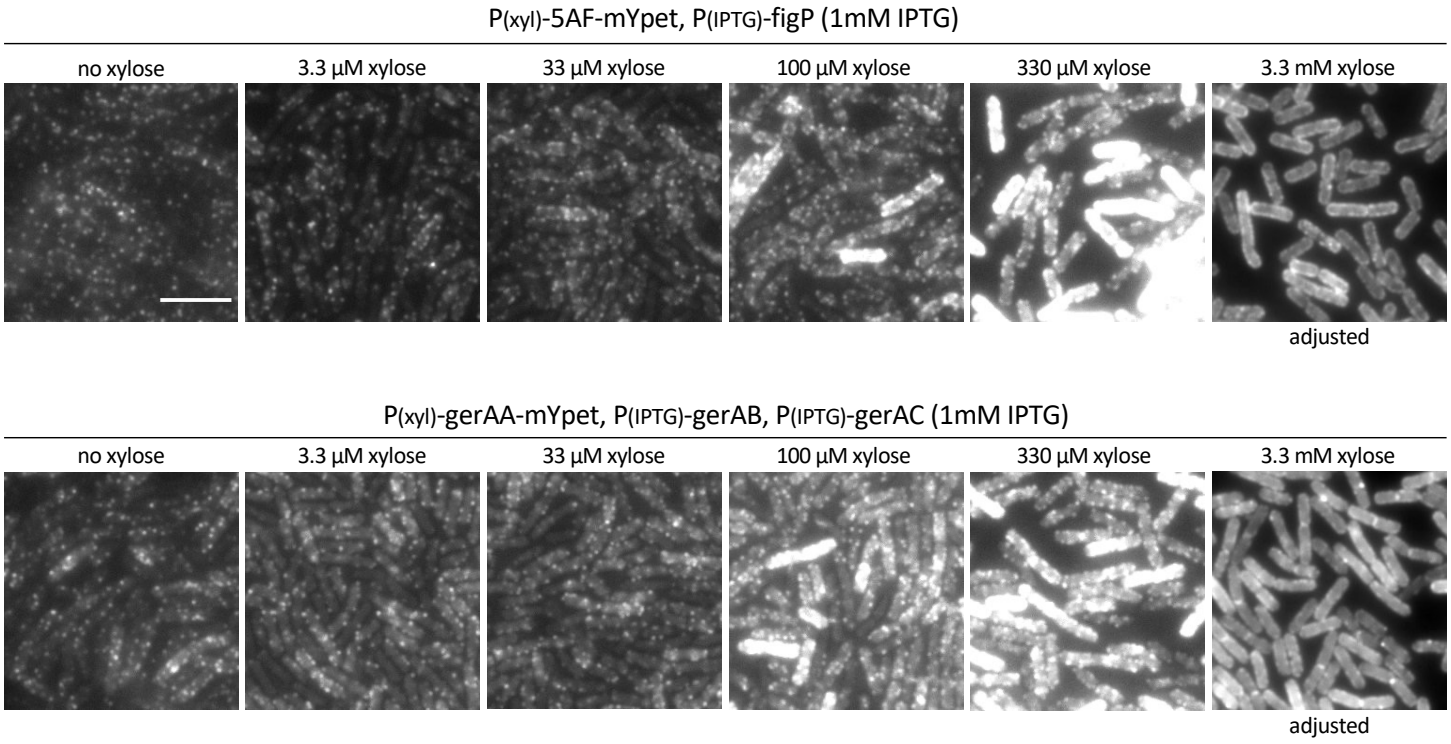


**Figure S14. 5FA-mYpet/FigP fluorescent foci are similar to GerAA-mYpet/GerAB/GerAC foci.**
Representative fluorescence images of vegetative cells expressing 5AF-mYpet or GerAA-mYpet in the presence of FigP or GerAB and GerAC, respectively. The mYpet fusions were expressed under the control of a xylose-regulated promoter ($P_{xylA}$) at the indicated concentrations. FigP, GerAB, and GerAC-His were expressed under the control of the IPTG-regulated promoter $P_{hyperspank}$ with 1 mM IPTG. All images were generated with the identical exposure time and are scaled identically, except those induced with 3.3 mM xylose, which were adjusted to detect the specific signal. Scale bar, 5 µm.

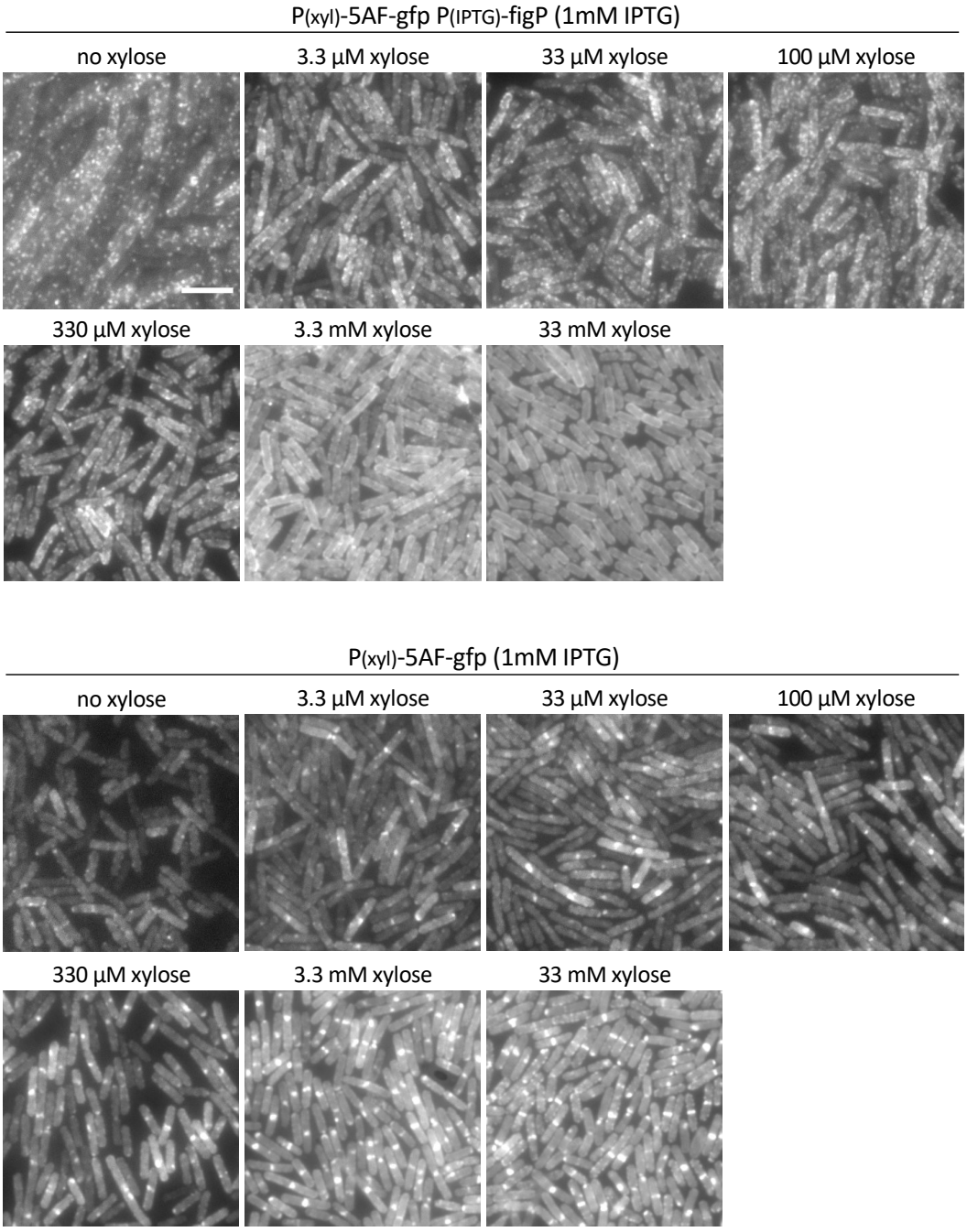


**Figure S15. 5AF-GFP fluorescent foci require expression of FigP.** Representative fluorescence images of vegetative cells expressing 5AF-GFP in the presence and absence of FigP. The 5AF-GFP fusion was expressed under the control of a xylose-regulated promoter ($P_{xylA}$) at the indicated concentrations. FigP was expressed under the control of the IPTG-regulated promoter $P_{hyperspank}$ with 1 mM IPTG. Scale bar, 5 µm. Each image was adjusted for the best visualization of 5AF-GFP.

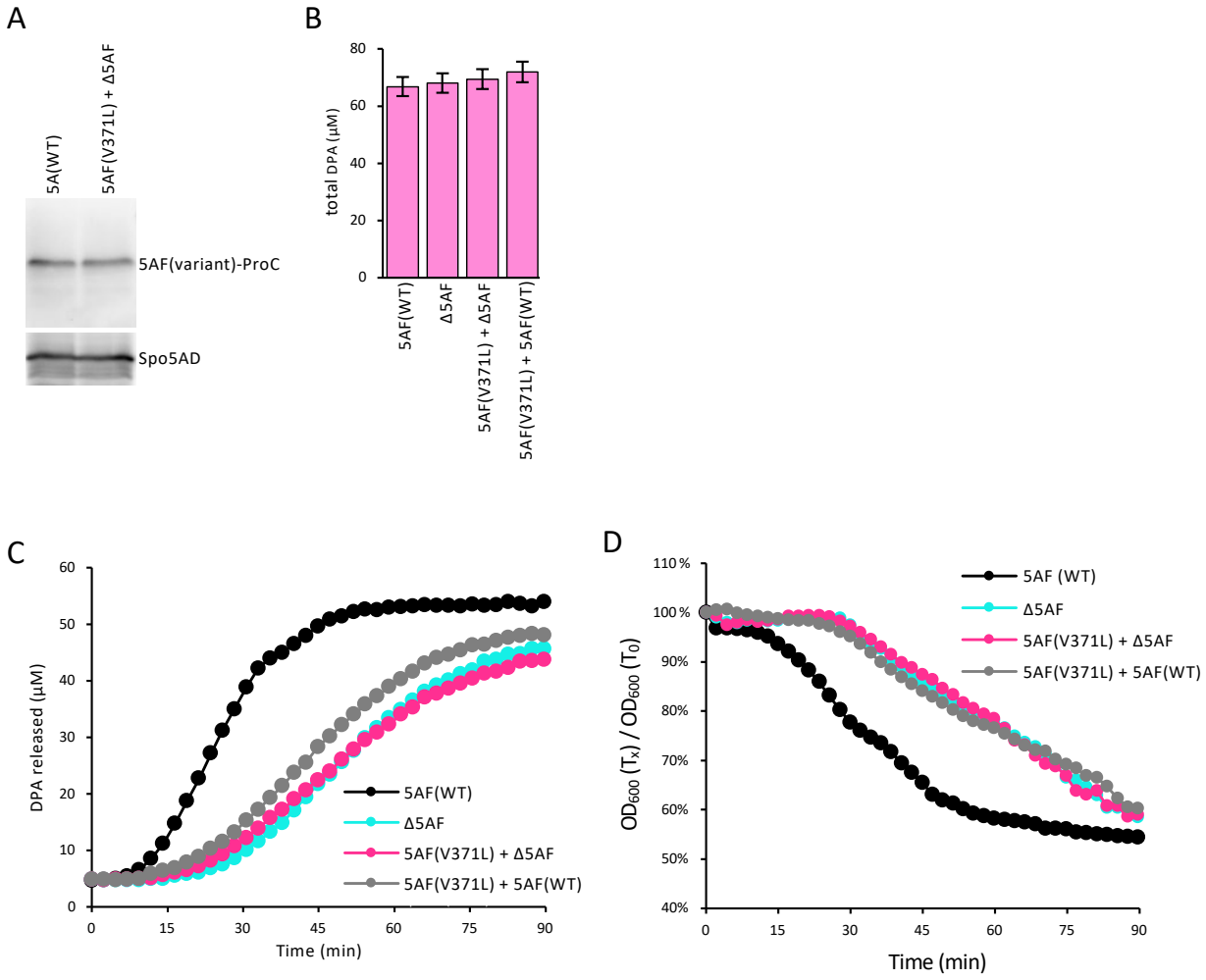


**Figure S16. GerAA(V371L) is strongly dominant-negative. (A)** Representative immunoblot monitoring the levels of 5AF variants in lysates from purified spores. For clarity, "5AF(WT)" was used throughout this figure to indicate that *5AF* is intact at its native locus. The levels of the 5AF-ProC variants were similar in spores harboring 5AF(V371L) at an ectopic locus in the absence of the native *5AF* gene and in spores with an intact *5AF* gene at its native locus ["5AF(WT)"]. **(B)** Bar graph showing total DPA in purified spores from the indicated strains are similar. **(C,D)** Purified spores from the indicated strains were mixed with 1 mM L-alanine and DPA release **(C)** and optical density **(D)** were monitored over time. Spores with equivalent levels of 5AF(WT) and the channel-narrowing mutant 5AF(V371L) were delayed in germination to an extent similar to Δ*5AF* and 5AF(V371L). These data support a model in which 5AF oligomerizes and the channel narrowing protomers can poison wild-type protomers.

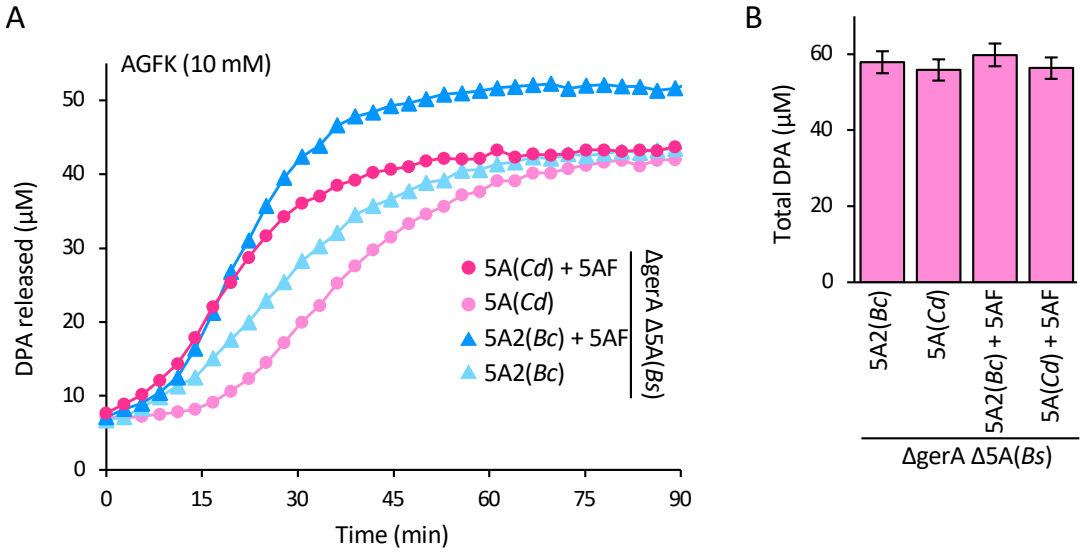


**Figure S17. 5AF enhances ion release by non-native DPA transport complexes. (A)** Purified spores from the indicated strains were mixed with 10 mM each of Asparagine, Glucose, Fructose, and $K^+$ (AGFK) and DPA release was monitored over time. Spores that contain 5AF release DPA faster than those that lack it. **(B)** Bar graph showing total DPA in purified spores from the indicated strains are similar.

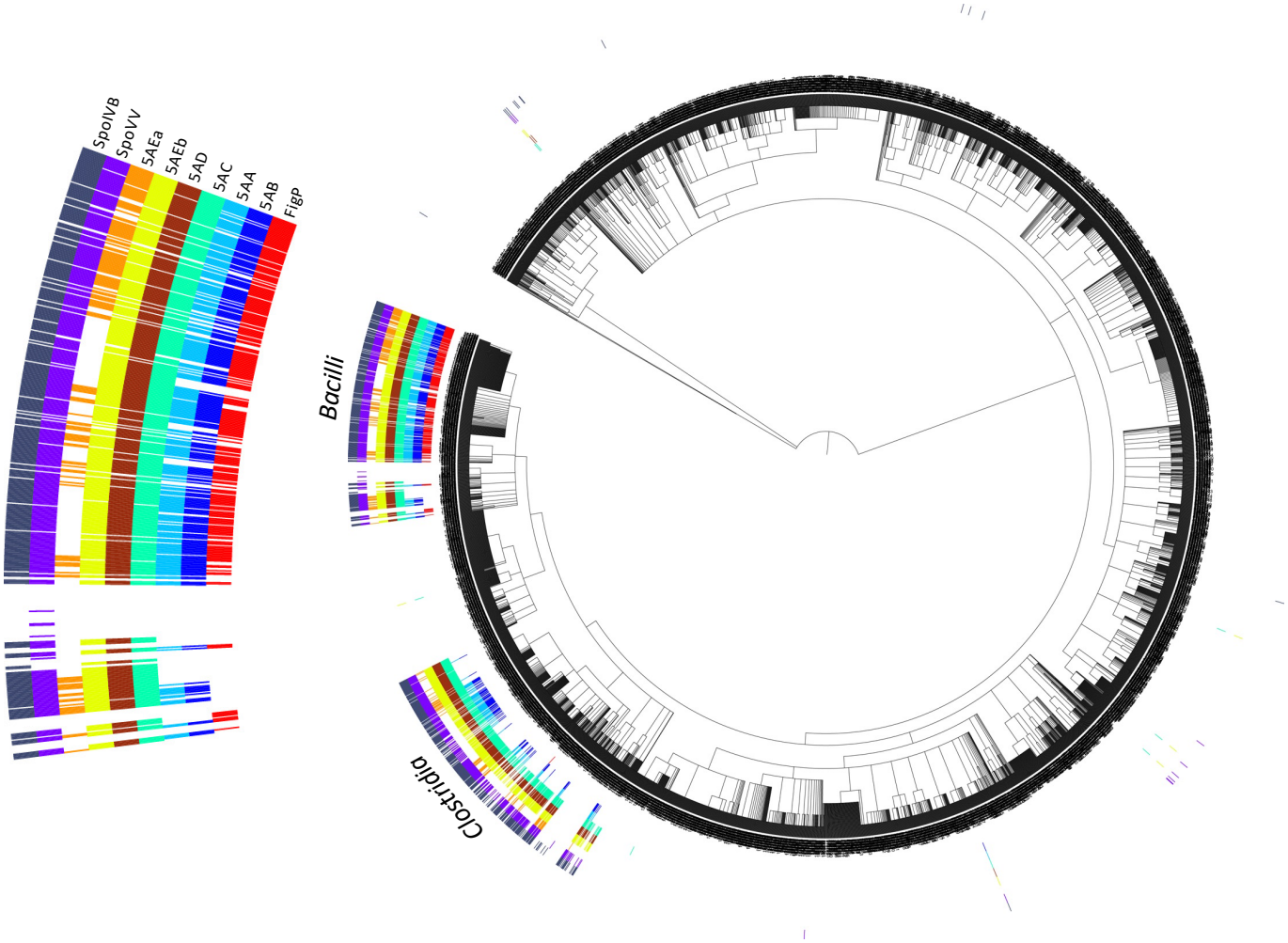


**Figure S18. FigP is conserved among *Bacilli*.** Occurrence of FigP across the bacterial phylogenetic tree. Red lines indicate the presence of a FigP homolog in the indicated species. Homologs of SpoIVB, SpoVV, and all the proteins encoded in the *spo5A* operon, with the exception of 5AF, are shown for comparison. 5AF was not included in this analysis because A subunits of GerA-family receptors are too similar to 5AF to distinguish between them. The NCBI nr database was searched using the *B. subtilis* FigP amino acid sequence or the other indicated proteins as the query. The BLASTp search program was used with an E-value cutoff of 0.001. The homologs were then plotted on a modified Newick tree built from Reference Prokaryotic Representative Genomes library available at NCBI (ftp.ncbi.nlm.nih.gov/blast/db). The tree was modified by removing duplicate species to generate unique taxID and scientific names for all organisms in the database. The phylogenetic tree was visualized in iTOL (http://phylot.biobyte.de).

Figure S19
*Gao et al.*

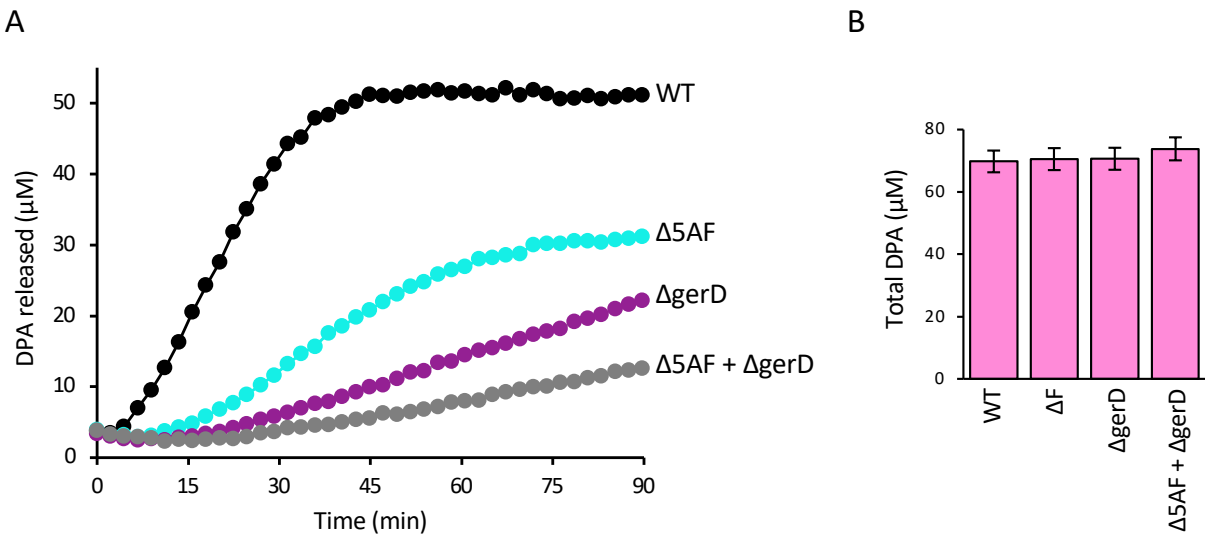


**Figure S19. 5AF enhances ion release in the absence of germinosomes. (A)** Purified spores from the indicated strains were mixed with 1 mM L-alanine and DPA release was monitored over time. Spores lacking 5AF or GerD were delayed in release of DPA. The double mutant was even more impaired, arguing that 5AF can act outside the germinosome. **(B)** Bar graph showing total DPA in purified spores from the indicated strains are similar.

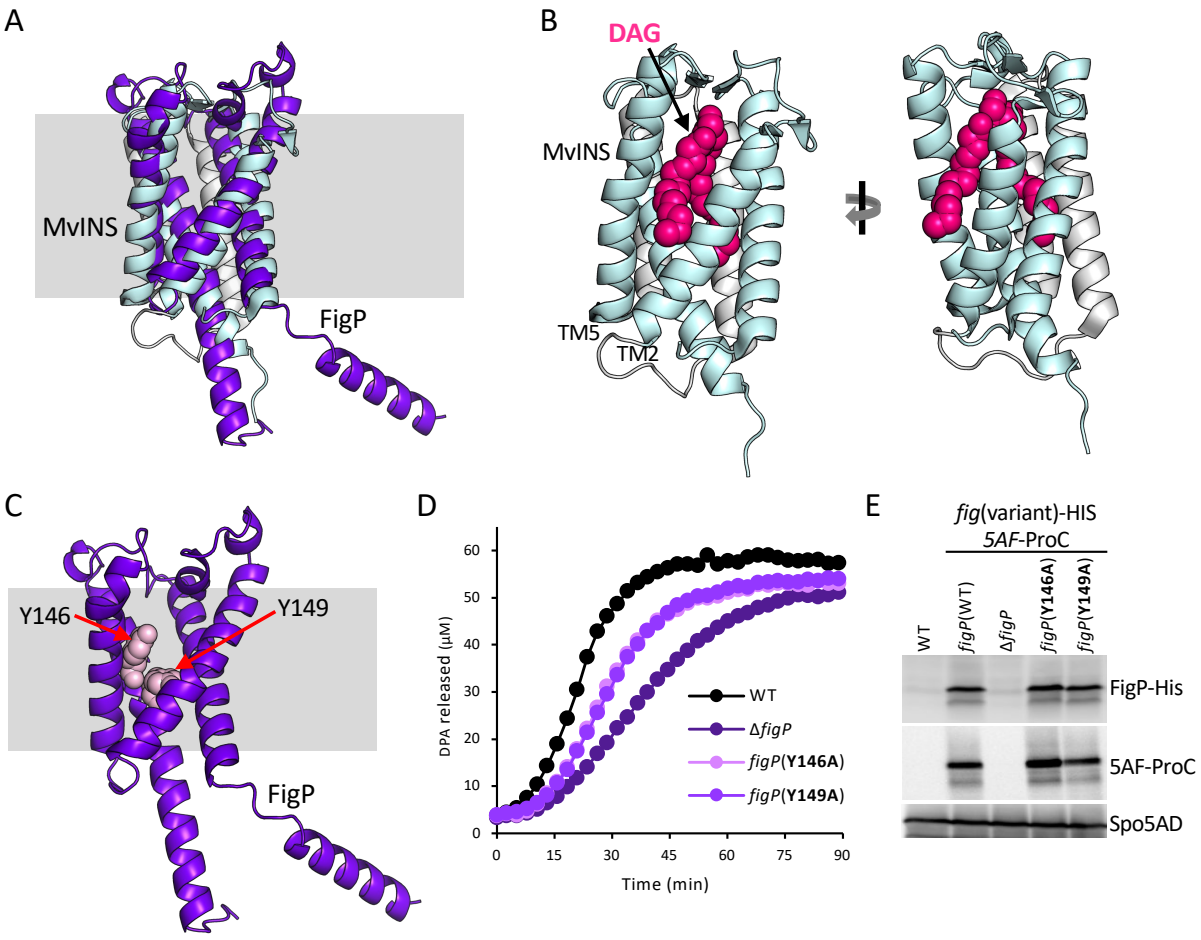


**Figure S20. The AlphaFold-predicted structure of FigP resembles INSIG homologs. (A)** Structural alignment by TM-align of the AlphaFold-predicted structure of FigP (purple) with the experimentally determined structure of the INSIG homolog from *Mycobacterium vanbaalenii* (MvINS) (PDB:4XU4). Transmembrane helices 3 and 4 of MvINS that are not present in FigP are shown in grey; the rest of the MvINS protein is in cyan. FigP is in purple. The TMalign score for the four TM segments of FigP and MvINS was 0.6 with an RMSD of 3.65 Å. **(B)** Structure of MvINS bound to diacylglycerol (DAG) in red (PDB:4XU5). **(C)** Predicted structure of FigP with conserved tyrosines (pink) that line the membrane pocket. **(D)** Purified spores from the indicated strains were mixed with 1 mM L-alanine and DPA release was monitored over time. Substitutions of Y146 or Y149 to alanine cause a partial delay in DPA release. **(E)** Immunoblot showing the levels of FigP-His and 5AF-ProC in dormant spores from the indicated strains. Spo5AD controls for loading. Spores lacking *figP* have undetectable levels of 5AF-ProC. FigP(Y146A) is stable in spores, while FigP(Y149A) levels are partially reduced. The FigP double mutant (Y146A, Y149A) was unstable and was not included in this analysis.

**Supplemental Table S1. Strains used in this study.**

| Strains | Genotype | Source | Figures |
|---|---|---|---|
| bAM860 | *ΔgerA::lox72 ΔgerBB::lox72 ΔgerKB::lox72 ΔyfkT::lox72 ΔyndE::lox72* | [1] | S2 |
| bDR2414 | *Bacillus subtilis 168 (trpC2) "wild-type"* | [2] | 1, 2, 3, S2, S3, S4, S8, S9, S10, S16, S19, S20 |
| bDR4332 | *ΔgerD::lox72* | This work | S19 |
| bLA219 | *ΔgerA::lox72 ΔgerBB::lox72 ΔgerKB::lox72 ΔyfkT::lox72 ΔyndE::lox72 lacA::PgerA-gerAC(erm) ycgO::PgerA-gerAB(spec) yhdG::PgerA-gerAA(tet)* | [1] | 5 |
| bYG08 | *ΔspoVAEa::lox72* | [3] | S2 |
| bYG09 | *ΔspoVAF::lox72* | [3] | 1, 2, 3, S2, S3, S4, S6, S8, S9, S10, S16, S19 |
| bYG1025 | *ΔspoVA::tet ycgO::PsspB-spoVA(Cd)(kan) yhdG::$P_{VA}$-spoVAF(spec)* | This work | 5 |
| bYG1066 | *ΔgerA::cat ΔspoVA::tet ycgO::PsspB-spoVA2(Bc)(kan) yhdG::$P_{VA}$-spoVAF(spec)* | This work | S17 |
| bYG1144 | *ΔspoVAF::lox72 ΔyqhR::lox72 ycgO::Phy-yqhR-His8(spec) yhdG::Pxyl-spoVAF-proC(phleo)* | This work | 3 |
| bYG1177 | *ΔspoVAF::lox72 ΔgerD::lox72* | This work | S19 |
| bYG1179 | *ΔgerA::lox72 ΔgerBB::lox72 ΔgerKB::lox72 ΔyfkT::lox72 ΔyndE::lox72 yvbJ::Phy-gerAC-His6(cat) ycgO::Phy-gerAB(spec) yhdG::Pxyl-gerAA-mYpet(phleo)* | This work | 4, S14 |
| bYG1184 | *ΔspoVAF::lox72 ΔyqhR::lox72 ycgO::Phy-yqhR-His6(spec) yhdG::Pxyl-spoVAF-proC(phleo) lacA::Pxyl-spoVAF-FLAG(erm)* | This work | 4 |
| bYG1201 | *ΔspoVAF::lox72 ΔyqhR::lox72 ycgO::Phy-yqhR-His8(spec) yhdG::Pxyl-spoVAF(phleo)* | This work | 3 |
| bYG1217 | *ΔspoVAF::lox72 yhdG::$P_{VA}$-spoVAF(V371L)(spec)* | This work | 2, S8, S16 |
| bYG1221 | *ΔspoVAF::lox72 yhdG::$P_{VA}$-spoVAF(Q375L)(spec)* | This work | 2, S8 |
| bYG1243 | *ΔspoVAF::lox72 ΔyqhR::lox72 yvbJ::yqhR-His8(kan)* | This work | 2 |
| bYG1246 | *ΔsleB::lox72 ΔspoVAF::lox72 yhdG::$P_{VA}$-spoVAF(V371L)-gfp(spec)* | This work | 2 |
| bYG1247 | *ΔsleB::lox72 ΔspoVAF::lox72 yhdG::$P_{VA}$-spoVAF(Q375L)-gfp(spec)* | This work | 2 |
| bYG1252 | *ΔspoVAF::lox72 ΔyqhR::lox72 yvbJ::yqhR-His8(Kan) yhdG::$P_{VA}$-spoVAF(V371L)-proC(spec)* | This work | 2 |
| bYG1253 | *ΔspoVAF::lox72 ΔyqhR::lox72 yvbJ::yqhR-His8(Kan) yhdG::$P_{VA}$-spoVAF(Q375L)-proC(spec)* | This work | 2 |
| bYG1255 | *ΔspoVAF::lox72 ΔyqhR::lox72 yvbJ::yqhR-His8(kan) yhdG::$P_{VA}$-spoVAF-proC(spec)* | This work | 2, S20 |
| bYG1265 | *ΔspoVAF::lox72 ΔyqhR::lox72 ycgO::Phy-yqhR-His6(spec) yhdG::Pxyl-spoVAF(phleo) lacA::Pxyl-spoVAF-FLAG(erm)* | This work | 4 |
| bYG1280 | *ΔspoVAF::lox72 ΔyqhR::lox72 yhdG::Pxyl-spoVAF-proC(phleo) lacA::Pxyl-spoVAF-FLAG(erm)* | This work | 4 |
| bYG1298 | *yhdG::$P_{VA}$-spoVAF(V371L)(spec)* | This work | S16 |
| bYG1309 | *ΔyqhR::lox72 yvbJ::yqhR(Y146A)(kan)* | This work | S20 |
| bYG1316 | *ΔyqhR::lox72 yvbJ::yqhR(Y149A)(kan)* | This work | S20 |
| bYG1324 | *ΔspoVAF::lox72 ΔyqhR::lox72 yhdG::$P_{VA}$-spoVAF-proC(spec)* | This work | S20 |
| bYG1334 | *ΔspoVAF::lox72 ΔyqhR::lox72 yhdG::$P_{VA}$-spoVAF-proC(spec) yvbJ::yqhR(Y146A)-His8(kan)* | This work | S20 |
| bYG1335 | *ΔspoVAF::lox72 ΔyqhR::lox72 yhdG::$P_{VA}$-spoVAF-proC(spec) yvbJ::yqhR(Y149A)-His8(kan)* | This work | S20 |
| bYG147 | *ΔspoVA::tet ycgO::PsspB-spoVA2(Bc)(kan)* | [1] | 5 |

| | | | |
|---|---|---|---|
| bYG1613 | *spoVAF-proC(phleo)* | This work | S16 |
| bYG1630 | *ΔspoVAF::lox72 yhdG::$P_{VA}$-spoVAF-ProC(spec)* | This work | S4 |
| bYG1664 | *ΔspoVAF::lox72 ΔyqhR::lox72 ycgO::Phy-yqhR(spec) yhdG::Pxyl-spoVAF-mYpet(phleo)* | This work | 4, S14, S15 |
| bYG1665 | *ΔspoVAF::lox72 ΔyqhR::lox72 yhdG::Pxyl-spoVAF-mYpet(phleo)* | This work | 4, S15 |
| bYG1667 | *ΔspoVAF::lox72 ΔyqhR::lox72 ycgO::Pveg-yqhR-His8(spec) yhdG::Phy-spoVAF-proC(erm)* | This work | 4 |
| bYG1683 | *ΔspoVAF::lox72 yhdG::$P_{VA}$-spoVAF(V371L)-proC(spec)* | This work | S16 |
| bYG1715 | *ΔspoVAF::lox72 ΔyqhR::lox72 yhdG::Phy-spoVAF-proC(erm)* | This work | 4 |
| bYG1716 | *ΔspoVAF::lox72 yhdG::$P_{VA}$-spoVAF-FLAG(spec)* | This work | S4 |
| bYG220 | *ΔsleB::lox72 ΔspoVAF::lox72 yhdG::$P_{VA}$-spoVAF-His8(spec)* | This work | 3 |
| bYG25 | *ΔspoVAF::lox72 yhdG::erm* | This work | S5 |
| bYG277 | *ΔspoVA::tet ycgO::PsspB-spoVA(Cd)(kan)* | [1] | 5 |
| bYG331 | *ΔspoVAF::lox72 yhdG::$P_{VA}$-spoVAF-gfp(spec)* | This work | S4, S6 |
| bYG358 | *ΔsleB::lox72 ΔspoVAF::lox72 yhdG::$P_{VA}$-spoVAF-gfp(spec)* | This work | 1, 2 |
| bYG382 | *ΔspoVAF::erm ΔgerA::lox72 ΔgerBB::lox72 ΔgerKB::lox72 ΔyfkT::lox72 ΔyndE::lox72 yhdG::$P_{VA}$-spoVAF-gfp(spec)* | This work | S6 |
| bYG383 | *ΔgerAB::lox72 ΔgerBB::lox72 ΔgerKB::lox72 ΔyfkT::lox72 ΔyndE::lox72 yhdG::PsspB-gerUA-gerUC-gerUB-gerVB(Bm) (spec)* | [1] | 5 |
| bYG390 | *ΔsleB::lox72 ΔspoVAF::lox72 yhdG::$P_{VA}$-spoVAF-gfp(spec) yvbJ::PgerA-gerAA-mScarlet(kan)* | This work | 1 |
| bYG403 | *ΔgerD::erm ΔsleB::lox72 ΔspoVAF::lox72 yhdG::$P_{VA}$-spoVAF-gfp(spec)* | This work | 1 |
| bYG417 | *ΔspoVA::tet ycgO::PsspB-spoVA2(Bc)(kan) yhdG::$P_{VA}$-spoVAF(spec)* | This work | 5 |
| bYG43 | *ΔspoVAF::lox72 yhdG::$P_{VA}$-spoVAF(spec)* | This work | 1, 2, S3, S4, S8 |
| bYG438 | *ΔspoVAF::erm ΔgerAB::lox72 ΔgerBB::lox72 ΔgerKB::lox72 ΔyfkT::lox72 ΔyndE::lox72 yhdG::PsspB-gerUA-gerUC-gerUB-gerVB(Bm)(spec)* | This work | 5 |
| bYG498 | *ΔsleB::lox72 ΔspoVAF::lox72 yhdG::$P_{VA}$-spoVAF(A360V)(spec)* | This work | S5 |
| bYG502 | *ΔsleB::lox72 ΔspoVAF::lox72 yhdG::$P_{VA}$-spoVAF(L367S)(spec)* | This work | S5 |
| bYG507 | *ΔspoVAF::lox72 yhdG::$P_{VA}$-spoVAF(A360V)(spec)* | This work | 2, S5, S6 |
| bYG511 | *ΔspoVAF::lox72 yhdG::$P_{VA}$-spoVAF(L367S)(spec)* | This work | 2, S5, S6 |
| bYG516 | *ΔsleB::lox72 ΔspoVAF::lox72 yhdG::erm* | This work | S5 |
| bYG519 | *ΔspoVAF::erm ΔgerA::lox72 ΔgerBB::lox72 ΔgerKB::lox72 ΔyfkT::lox72 ΔyndE::lox72* | This work | S2, S6 |
| bYG530 | *ΔspoVAF::erm ΔgerA::lox72 ΔgerBB::lox72 ΔgerKB::lox72 ΔyfkT::lox72 ΔyndE::lox72 yhdG::$P_{VA}$-spoVAF(A360V)* | This work | S6 |
| bYG540 | *ΔspoVAF::erm ΔgerA::lox72 ΔgerBB::lox72 ΔgerKB::lox72 ΔyfkT::lox72 ΔyndE::lox72 yhdG::$P_{VA}$-spoVAF(L367S)(spec)* | This work | S6 |
| bYG57 | *ΔspoVAF::lox72 yhdG::$P_{VA}$-spoVAF-His8(spec)* | This work | S4 |
| bYG584 | *ΔspoVAF::lox72 ycgO::$P_{VA}$-spoVAF(A360V)(cat)* | This work | 3, S9 |
| bYG611 | *ΔgerA::cat ΔspoVA::tet ycgO::PsspB-spoVA(Cd)(kan) yhdG::$P_{VA}$-spoVAF(spec)* | This work | S17 |
| bYG701 | *ΔyktB::lox72* | This work | S9, S10 |
| bYG702 | *ΔymfJ::lox72* | This work | S9, S10 |
| bYG703 | *ΔytpA::lox72* | This work | S9, S10 |
| bYG704 | *ΔymfD::lox72* | This work | S9, S10 |
| bYG705 | *ΔyqhR::lox72* | This work | 3, S9, S20 |
| bYG706 | *ΔyqhR ΔspoVAF::lox72 ycgO::$P_{VA}$-spoVAF(A360V)(cat)* | This work | 3 |
| bYG711 | *ΔspoVAF::lox72 ΔymfD::lox72* | This work | S10 |
| bYG712 | *ΔspoVAF::lox72 ΔymfJ::lox72* | This work | S10 |
| bYG713 | *ΔspoVAF::lox72 ΔyktB::lox72* | This work | S10 |

| | | | |
|---|---|---|---|
| bYG714 | *ΔspoVAF::lox72 ΔytpA::lox72* | This work | S10 |
| bYG715 | *ΔspoVAF::lox72 ΔyqhR::lox72* | This work | 3 |
| bYG725 | *ΔyqhR::lox72 ΔspoVAF::lox72 ycgO::$P_{VA}$-spoVAF(A360V)(cat)* | This work | S9 |
| bYG726 | *ΔytpA::lox72 ΔspoVAF::lox72 ycgO::$P_{VA}$-spoVAF(A360V)(cat)* | This work | S9 |
| bYG727 | *ΔyktB::lox72 ΔspoVAF::lox72 ycgO::$P_{VA}$-spoVAF(A360V)(cat)* | This work | S9 |
| bYG728 | *ΔymfJ::lox72 ΔspoVAF::lox72 ycgO::$P_{VA}$-spoVAF(A360V)(cat)* | This work | S9 |
| bYG729 | *ΔymfD::lox72 ΔspoVAF::lox72 ycgO::PVA-spoVAF(A360V)(cat)* | This work | S9 |
| bYG783 | *ΔgerA::cat ΔspoVA::tet ycgO::PsspB-spoVA2(Bc)(kan)* | This work | S17 |
| bYG785 | *ΔsleB::lox72 ΔyqhR::lox72 yvbJ::yqhR-His8(kan)* | This work | 3 |
| bYG788 | *ΔsleB::lox72 ΔspoVAF::lox72 ΔyqhR::lox72 yvbJ::yqhR-His8(kan)* | This work | 3 |
| bYG793 | *ΔgerA::cat* | This work | 2, S8 |
| bYG795 | *ΔsleB::lox72 ΔspoVAF::lox72 ΔyqhR::erm yhdG::$P_{VA}$-spoVAF-His8(spec)* | This work | 3 |
| bYG797 | *ΔgerA::cat ΔspoVA::tet ycgO::PsspB-spoVA(Cd)(kan)* | This work | S17 |
| bYG802 | *ΔsleB::lox72 ΔspoVAF::lox72 ΔyqhR::lox72 yhdG::$P_{VA}$-spoVAF-gfp(spec) yvbJ::yqhR-mScarlet(kan)* | This work | 3 |
| bYG879 | *ΔspoVAF::lox72 ΔyqhR::lox72 ycgO::Pveg-yqhR(spec) yhdG::Phy-spoVAF(erm)* | This work | 4, S13 |
| bYG881 | *ΔspoVAF::lox72 ΔyqhR::lox72 ycgO::Pveg-yqhR(spec) yhdG::Phy-spoVAF(L367S)(erm)* | This work | 4, S13 |
| bYG882 | *ΔspoVAF::lox72 ΔyqhR::lox72 yhdG::Phy-spoVAF(erm)* | This work | 4 |
| bYG884 | *ΔspoVAF::lox72 ΔyqhR::lox72 yhdG::Phy-spoVAF(L367S)(erm)* | This work | 4, S13 |

**Supplemental Table S2. Plasmids used in this study.**

| Plasmid | Genotype | Source |
|---|---|---|
| pCOLADuet-1 | Expression vector with two T7 promoters; COLA replicon, (*kan*) | Novagen |
| pFR38 | Himar1 C9 transposase, ITR2-*spec*-ITR1(MmeI site in ITR1) (*erm*) | laboratory stock |
| pLA73 | *MCS-proC His-SUMO-FLAG-MCS (amp)* | [4] |
| pCB179 | *yhdG::$P_{VA}$ (spec)(amp)* | [3] |
| pDR244 | *cre (spec)(amp)* | laboratory stock |
| pWX318 | *mYpet (cat) (amp)* | laboratory stock |
| pCB47 | *yvbJ::kan (amp)* | laboratory stock |
| pCB42 | *ycgO::cat (amp)* | laboratory stock |
| pCB47 | *yvbJ::kan (amp)* | laboratory stock |
| pLA155 | *ycgO::Pveg-gerAB (spec)(amp)* | [1] |
| pCB100 | *yhdG::Phypespank(hy) (erm)(amp)* | laboratory stock |
| pCB90 | *ycgO:: Phy (spec)(amp)* | laboratory stock |
| pCB109 | *yhdG::PxylA (phleo)(amp)* | laboratory stock |
| pDR183 | *lacA::erm (amp)* | laboratory stock |
| pYG47 | *ycgO::$P_{VA}$-spoVAEb(cat)(amp)* | [1] |
| pYG07 | *yhdG::$P_{VA}$ -spoVAF (spec)(amp)* | This study |
| pYG31 | *yhdG::$P_{VA}$-spoVAF-His8 (spec)(amp)* | This study |
| pYG105 | *yhdG::$P_{VA}$-spoVAF-gfp (spec)(amp)* | This study |
| pYG137 | *yvbJ::PgerA-gerAA-mScarlet (kan)(amp)* | This study |
| pYG156 | *spoVAF (kan)* | This study |
| pYG228 | *ycgO::$P_{VA}$-spoVAF (cat)(amp)* | This study |
| pYG189 | *ycgO::$P_{VA}$-spoVAF(A360V) (cat)(amp)* | This study |
| pYG235 | *yvbJ::yqhR-mScarlet (kan)(amp)* | This study |
| pYG238 | *yvbJ::yqhR-His8 (kan)(amp)* | This study |
| pYG269 | *ycgO::Pveg-yqhR (spec)(amp)* | This study |
| pYG270 | *yhdG::Phy-spoVAF (erm)(amp)* | This study |
| pYG272 | *yhdG::Phy-spoVAF(L367S) (erm)(amp)* | This study |
| pYG293 | *ycgO::$P_{VA}$-spoVAF(L367S) (cat)(amp)* | This study |
| pYG296 | *ycgO::Pveg-yqhR-His8 (spec)(amp)* | This study |
| pYG297 | *spoVAF-proC (amp)* | This study |
| pYG314 | *ycgO::Phy-yqhR (spec)(amp)* | This study |
| pYG318 | *yhdG::Pxyl-spoVAF-proC (phleo)(amp)* | This study |
| pYG319 | *ycgO::Phy-yqhR-His8 (spec)(amp)* | This study |
| pYG341 | *yhdG::$P_{VA}$-spoVAF-proC (spec)(amp)* | This study |
| pYG563 | *yhdG::$P_{VA}$-spoVAF-FLAG (spec)(amp)* | This study |
| pYG351 | *lacA::Pxyl-spoVAF-FLAG (erm)(amp)* | This study |
| pYG360 | *yhdG::Pxyl-spoVAF (phleo)(amp)* | This study |
| pYG377 | *yhdG::$P_{VA}$-spoVAF(V371L) (spec)(amp)* | This study |
| pYG378 | *yhdG::$P_{VA}$-spoVAF(Q375L) (spec)(amp)* | This study |
| pYG386 | *yhdG::$P_{VA}$-spoVAF(V371L)-gfp (spec)(amp)* | This study |
| pYG387 | *yhdG::$P_{VA}$-spoVAF(Q375L)-gfp (spec)(amp)* | This study |
| pYG388 | *yhdG::$P_{VA}$-spoVAF(V371L)-proC (spec)(amp)* | This study |
| pYG389 | *yhdG::$P_{VA}$-spoVAF(Q375L)-proC (spec)(amp)* | This study |
| pYG415 | *yvbJ::PyqhR-yqhR (kan)(amp)* | This study |
| pYG416 | *yvbJ::PyqhR-yqhR(Y146A) (kan)(amp)* | This study |
| pYG417 | *yvbJ::PyqhR-yqhR(Y149A) (kan)(amp)* | This study |

| | | |
|---|---|---|
| pYG432 | *yvbJ::PyqhR-yqhR(Y146A)-His8 (kan)(amp)* | This study |
| pYG433 | *yvbJ::PyqhR-yqhR(Y149A)-His8 (kan)(amp)* | This study |
| pYG540 | *yhdG::Pxyl-spoVAF-mYpet (phleo)(amp)* | This study |
| pYG546 | *yhdG::Phy-spoVAF-proC (erm)(amp)* | This study |

**Supplemental Table 3. Oligonucleotides used in this study.**

| oligos | sequence | use |
|---|---|---|
| oYG17 | TGCCAGTCACGTTACGTTATTAG | sequence *spoVAF* |
| oYG380 | CAGTGCAGGCTAGCTTTTTTG | sequence *spoVAF* |
| oCB63 | gactggtttttgctcagacaa | amplify *spoVAF* mutants |
| oYG381 | CCACTCTCAACTCCTGATCCAAACA | amplify *spoVAF* mutants |
| oYG1048 | ATGTATTCACGAACGAAAATCGCCTACTTATCATCATCATCCTTATAGTCgga | pYG563 |
| oYG109 | GCGATTTTCGTTCGTGAATACATGT | pYG105, pYG341, pYG563 |
| oYG110 | ctggcggaagcggaggatccAAGGGAGAAGAGTTGTTTACGGGT | pYG105 |
| oYG111 | GTATTCACGAACGAAAATCGCTTaggtgctACTAGTAGAACCACCGCCT | pYG105 |
| oYG190 | CATCCATGgtatatctccttcttaaagttaaac | pYG297 |
| oYG20 | CACcatcatCACCACcatcatCACTAGGCGATTTTCGTTCGTGAATACATGT | pYG31 |
| oYG27 | tgatgGTGGTGatgatgGTGTGAATTGGTAGGCTGCCTTAAGCGA | pYG31 |
| oYG282 | ggatcctccgcttccgccagagcctccTGAATTGGTAGGCTGCCTTAAGCGA | pYG105, pYG297, pYG540 |
| oYG292 | GAATTCGACATCAAGAGCGGGAAGGGAGATTTG | pYG137, pYG235, pYG238, pYG415 |
| oYG293 | CTCGAGatGCTAGCatGGATCCcagc | pYG137, pYG235, pYG415 |
| oYG35 | cagcgACTAGTTTTATTTTAGAAAGGAGCGGGTATC | pYG07 |
| oYG351 | TCCCGCTCTTGATGTCGAATTCGTCCTGCCGTACTCCTTTGATGT | pYG137 |
| oYG352 | ggatcctccgcttccgccagagcctccAGTTTCAGTGGAGTCTGTTTTTG | pYG137 |
| oYG353 | ctggcggaagcggaggatccGTTTCGAAAGGTGAGGCAGTTATTAAG | pYG137, pYG235 |
| oYG354 | GATCCatGCTAGCatCTCGAGttaCTTGTACAGTTCATCCATGCCGCCGGT | pYG137, pYG235 |
| oYG36 | cacggCTCGAGTTATGAATTGGTAGGCTGCCTTAAG | pYG07 |
| oYG392 | atggctgctgcccatggtatatc | pYG156 |
| oYG393 | ctcgagtctggtaaagaaaccgct | pYG156 |
| oYG394 | ataccatgggcagcagccatTTTATTTTAGAAAGGAGCGGGTATCATG | pYG156 |
| oYG395 | ggtttctttaccagactcgagTACTCTTCAGTCAGTTTCAATGCGA | pYG156 |
| oYG396 | ACTAGTatAAGCTTtcggtggttatatatgtaGTATGTGGTTCGA | pYG189, pYG228, pYG293 |
| oYG397 | ccaccgaAAGCTTatACTAGTTTTATTTTAGAAAGGAGCGGGTATCATG | pYG189, pYG228, pYG293 |
| oYG398 | GATCCatGCTAGCatCTCGAGTACTCTTCAGTCAGTTTCAATGCGA | pYG189, pYG228, pYG293 |
| oYG417 | catatataaccaccgaAAGCTTatACTAGTTTTATTTTAGAAAGGAGCGGGTATCATG | *spoVAF* PCR mutagenesis |
| oYG418 | CAGGGGGATCCatGCTAGCatCTCGAGTACTCTTCAGTCAGTTTCAATGCGA | *spoVAF* PCR mutagenesis |
| oYG437 | CTCGAGatGCTAGCatGGATCCCATAC | pYG189, pYG228, pYG293 |
| oYG534 | CTACTTATCATCATCATCCTTATAGTCggatcctccgcttccgccagagc | pYG351 |
| oYG551 | TCCCGCTCTTGATGTCGAATTCATCCGTTCTTCTGATGGCTGTAAC | pYG235, pYG238, pYG415 |
| oYG552 | ggatcctccgcttccgccagagcctccTTCTCTATGCATTCCCAGCGCACGT | pYG235 |
| oYG561 | CACcatcatCACCACcatcatCACTAACTCGAGatGCTAGCatGGATCCcagc | pYG238 |
| oYG562 | TTAGTGatgatgGTGGTGatgatgGTGggatcctccgcttccgccagagc | pYG238, pYG296 |
| oYG604 | ttggattattcacctcttttggttACTAGTcact | pYG269, pYG296 |

| | | |
|---|---|---|
| oYG605 | GGATCCTTCTGCTCCCTCGCTCAG | pYG269 |
| oYG606 | ccaaaagaggtgaataatccaaATGATGACAAGCGAAAAAGATACAG | pYG269, pYG296 |
| oYG607 | GAGCGAGGGAGCAGAAGGATCCCTATTCTCTATGCATTCCCAGCGCACGT | pYG269 |
| oYG608 | GtAATTGTGAGCGGATAACAATTAAGCTTTTTATTTTAGAAAGGAGCGGGTATCATG | pYG270, pYG272, pYG546 |
| oYG609 | TGCgaGCTAGCatCTGCAGttACTAGTTTATGAATTGGTAGGCTGCCTTAAG | pYG270, pYG272 |
| oYG618 | GCgaGCTAGCatCTGCAGttATCACTTCCCATCAATGAGCCGCGGATCTACTTGGTC | pYG546 |
| oYG637 | CACcatcatCACCACcatcatCACTAAGGATCCTTCTGCTCCCTCGCTCAG | pYG296 |
| oYG638 | gtttaactttaagaaggagatataccatggATGCCGGACCACAAGGAAGAGAAAATTC | pYG297 |
| oYG661 | tctggcggaagcggaggatccACTAGTGAAGACCAAGTAGATCCGCGGCT | pYG297 |
| oYG664 | GtAATTGTGAGCGGATAACAATTAaaccaaaagaggtgaataatccaaATGA | pYG314, pYG319 |
| oYG665 | TGCgaGCTAGCatCTGCAGttACTATTCTCTATGCATTCCCAGCGCACGT | pYG314 |
| oYG667 | taacctgaagAATTgGATCCatCTCACTTCCCATCAATGAGCCGCGGATCTACTTGGTC | pYG318 |
| oYG668 | TTTATTTTAGAAAGGAGCGGGTATCATGCCGGACCACAAGGAAGAGAAAATTC | pYG318 |
| oYG669 | gaaataaaatgcatctgtatttgaatgATTTATTTTAGAAAGGAGCGGGTATCATG | pYG318, pYG360 |
| oYG670 | TGCgaGCTAGCatCTGCAGttATTAGTGatgatgGTGGTGatgatgGTGgga | pYG319 |
| oYG703 | ATGTATTCACGAACGAAAATCGCTCACTTCCCATCAATGAGCCGCGGATCTACTTGGTC | pYG341 |
| oYG726 | GAACGTCCCGGGGAGCTCatgCGTGCCATGTCACTATTGCTTCAGAAATAC | pYG351 |
| oYG727 | cctagcatgcatgctagcatcCTACTTATCATCATCATCCTTATAGTCgga | pYG351 |
| oYG737 | GGATCcAATTcttcaggttatgaccatctgtgccag | pYG540 |
| oYG738 | tctggcggaagcggaggatccTCAAAAGGCGAAGAGCTGTTTACCGGAG | pYG540 |
| oYG739 | gtcataacctgaagAATTgGATCCTTACTTGTAAAGTTCATTCATCCCTTCTGT | pYG540 |
| oYG74 | ttCCTCCTTAtgttcggtggttatatatgtaGTATGTGGTTCGA | pYG31, pYG341, pYG563 |
| oYG740 | taacctgaagAATTgGATCCatCTTATGAATTGGTAGGCTGCCTTAAGCGA | pYG360 |
| oYG75 | accaccgaacaTAAGGAGGaactactATGCCGGACCACAAGGAAGAGA | pYG31, pYG341, pYG563 |
| oYG750 | AGCAATGGGTTTAATTGCCGCTCTTCTGATCGGGCAGATTGCGA | pYG377, pYG386, pYG388 |
| oYG751 | TCGCAATCTGCCCGATCAGAAGAGCGGCAATTAAACCCATTGCT | pYG377, pYG386, pYG388 |
| oYG752 | TGCCGCTGTTCTGATCGGGCTGATTGCGATTGAGGTCGGCCT | pYG378, pYG387, pYG389 |
| oYG753 | AGGCCGACCTCAATCGCAATCAGCCCGATCAGAACAGCGGCA | pYG378, pYG387, pYG389 |
| oYG799 | tgGGATCCatGCTAGCatCTCGAGCTATTCTCTATGCATTCCCAGCGCACGT | pYG415 |
| oYG800 | CAATTATTACGACCATTTGCATTGCTTTGCTTTACGGGCTGTTTGTC | pYG416, pYG432 |
| oYG801 | GACAAACAGCCCGTAAAGCAAAGCAATGCAAATGGTCGTAATAATTG | pYG416, pYG432 |
| oYG802 | ACCATTTGCATTTATTTGCTTGCCGGGCTGTTTGTCGGGTATTC | pYG417, pYG433 |
| oYG803 | GAATACCCGACAAACAGCCCGGCAAGCAAATAAATGCAAATGGT | pYG417, pYG433 |

**Supplemental Methods**

**Plasmid constructions**

**pYG07[*yhdG::$P_{VA}$-spoVAF(spec)(amp)*]** was constructed in a 2-way ligation with a PCR product containing the *spoVAF* gene amplified with oYG35 and oYG36 using gDNA of *B. subtilis 168*, and the plasmid pCB179 cut with SpeI and XhoI. pCB179 is a double crossover integration vector at the *yhdG* locus with a *spec* cassette and the promoter of *spoVA* operon ($P_{VA}$).

**pYG31[*yhdG::$P_{VA}$-spoVAF-His8(spec)(amp)*]** was constructed in a 2-way isothermal assembly reaction with a PCR product containing *spoVAF-His8* amplified with primers oYG75 and oYG27 using gDNA of *B. subtilis 168*, and the plasmid pCB179 amplified with primers oYG20 and oYG74. pCB179 is a double crossover integration vector at *yhdG* locus with a *spec* cassette and the promoter of *spoVA* operon ($P_{VA}$).

**pYG105[*yhdG::$P_{VA}$-spoVAF-gfp(spec)(amp)*]** was constructed in a 2-way isothermal assembly reaction with a PCR product containing *gfp* amplified with primers oYG110 and oYG111 using plasmid pHCL132 (laboratory stock), and plasmid pYG31 amplified with oYG109 and oYG282.

**pYG137[*yvbJ::PgerA-gerAA-mScarlet(kan)(amp)*]** was constructed in a 3-way isothermal assembly reaction with 2 PCR products and pCB47 amplified with oYG292 and oYG293. One PCR product containing *PgerA-gerAA* was amplified with oYG351 and oYG352 using gDNA of *B. subtilis 168*, and another PCR product containing mScarlet was derived from pCB142 (laboratory stock) with primers oYG353 and oYG354. pCB47 is a double crossover integration vector at *yvbJ* locus with a *kan* cassette.

**pYG156[*spoVAF(kan)*]** was constructed in a 2-way isothermal assembly reaction with a PCR product containing *spoVAF* amplified with oYG394 and oYG395 using gDNA of *B. subtilis 168*, and plasmid pCOLADuet-1(Novagen) amplified with oYG393 and oYG394. pYG156 was used as a template for PCR mutagenesis of *spoVAF*.

**pYG189[*ycgO::$P_{VA}$-spoVAF(A360V)(cat)(amp)*]** was constructed in a 2-way isothermal assembly reaction with a PCR product containing *spoVAF(A360V)* amplified with oYG397 and oYG398 using gDNA of bYG498, and the plasmid pYG47 [3] amplified with oYG396 and oYG437.

**pYG293[*ycgO::$P_{VA}$-spoVAF(L367S)(cat)(amp)*]** was constructed in a 2-way isothermal assembly reaction with a PCR product containing *spoVAF(L367S)* amplified with oYG397 and oYG398 using gDNA of bYG502, and the plasmid pYG47 [3] amplified with oYG396 and oYG437.

**pYG228[*ycgO::$P_{VA}$-spoVAF(cat)(amp)*]** was constructed in a 2-way isothermal assembly reaction with a PCR product containing *spoVAF* amplified with oYG397 and oYG398 using gDNA of *B. subtilis 168*, and the plasmid pYG47 [3] amplified with oYG396 and oYG437.

**pYG235[*yvbJ::yqhR-mScarlett(kan)(amp)*]** was constructed in a 3-way isothermal assembly reaction with 2 PCR products and pCB47 amplified with oYG292 and oYG293. One PCR product contained the *yqhR* gene with its native promoter amplified with primers oYG551 and oYG552 using gDNA of *B. subtilis 168,* the second PCR product contained *mScarlet* derived from pCB142 (laboratory stock) with primers oYG353 and oYG354. pCB47 is a double crossover integration vector at *yvbJ* locus with a *kan* cassette.

**pYG238[*yvbJ::yqhR-His8(kan)(amp)*]** was constructed in a 2-way isothermal assembly reaction with a PCR product contained the *yqhR* gene with its native promoter amplified with oYG551 and oYG562 using pYG235 as template, and plasmid pCB47 amplified with oYG561 and oYG292. pCB47 is a double crossover integration vector at *yvbJ* locus with a *kan* cassette.

**pYG269[*ycgO::Pveg-yqhR(spec)(amp)*]** was constructed in a 2-way isothermal assembly reaction with a PCR product containing the *yqhR* amplified with oYG606 and oYG607 using gDNA of *B. subtilis 168,* and plasmid pLA155 [1] amplified with oYG604 and oYG605.

**pYG296[*ycgO::Pveg-yqhR-His8(spec)(amp)*]** was constructed in a 2-way isothermal assembly reaction with a PCR product containing the gene *yqhR* amplified with oYG606 and oYG562 using pYG235 as template, and plasmid pLA155 [1] amplified with oYG604 and oYG637.

**pYG270[*yhdG::Phy-spoVAF(erm)(amp)*]** was constructed in a 2-way isothermal assembly reaction with a PCR product containing s*poVAF* amplified with oYG608 and oYG609 using gDNA of *B. subtilis 168*, and the plasmid pCB100 cut with HindIII and SpeI. pCB100 is a double crossover integration vector at the *yhdG* locus with an *erm* cassette and the IPTG-inducible promoter Phyperspank (laboratory stock).

**pYG272[*yhdG::Phy-spoVAF(L367S)(erm)(amp)*]** was constructed in a 2-way isothermal assembly reaction with a PCR product containing *spoVAF(L367S)* amplified with primers oYG608 and oYG609 using gDNA of bYG502, and the plasmid pCB100 cut with HindIII and SpeI. pCB100 is a double crossover integration vector at the *yhdG* locus with an *erm* cassette and the IPTG-inducible promoter Phyperspank (laboratory stock).

**pYG314[*ycgO::Phy-yqhR(spec)(amp)*]** was constructed in a 2-way isothermal assembly reaction with a PCR product containing *yqhR* amplified with oYG664 and oYG665 using pYG269, and plasmid cut with pCB90 cut with HindIII and SpeI. pCB100 is a double crossover integration vector at the *yhdG* locus with an *erm* cassette and the IPTG-inducible promoter Phyperspank (laboratory stock).

**pYG297[*spoVAF-proC (amp)*]** was constructed in a 2-way isothermal assembly reaction with a PCR product containing *spoVAF* with primers oYG638 and oYG282 using gDNA of *B. subtilis 168*, and plasmid pLA73 amplified with oYG661 and oYG190. pLA73 is a plasmid used for protein expression in *E. coli* carrying the ProteinC (ProC) and FLAG epitope tags.

**pYG318[*yhdG::PxylA-spoVAF-proC(phleo)(amp)*]** was constructed in a 2-way isothermal assembly reaction with a PCR product containing *spoVAF-proC* and plasmid pCB109 cut with HindIII and XhoI. The PCR product was first amplified with primers oYG667 and oYG668 using plasmid pYG297 as template, and subsequently, amplified with oYG667 and oYG669 using the initial PCR product as a template. pCB109 is a double crossover integration vector at the *yhdG* locus with a *phleo* cassette and a xylose-inducible promoter P*xylA* (laboratory stock).

**pYG319[*ycgO::Phy-yqhR-His8(spec)(amp)*]** was constructed in a 2-way isothermal assembly reaction with a PCR product containing *yqhR-His8* amplified with primers oYG664 and oYG670 using pYG296 as template, and plasmid pCB90 cut with HindIII and SpeI. pCB90 is a double crossover integration vector at *ycgO* locus with a *spec* cassette and the IPTG-inducible promoter Phyperspank (laboratory stock).

**pYG341[*yhdG::$P_{VA}$-spoVAF-proC(spec)(amp)*]** was constructed in a 2-way isothermal assembly reaction with a PCR product containing *spoVAF-proC* amplified with oYG75 and oYG703 using pYG318

as template, and plasmid pCB179 amplified with oYG74 and oYG109. pCB179 is a double crossover integration vector at *yhdG* locus with a *spec* cassette and the promoter of the *spoVA* operon ($P_{VA}$).

**pYG351[*lacA::PxylA-spoVAF-FLAG(erm)(amp)*]** was constructed in a 2-way isothermal assembly reaction with a PCR product containing the *spoVAF-FLAG* and plasmid pdr183 cut with EcoRI and XhoI. The PCR product was first amplified with oYG534 and oYG726 using pYG318 as template, and subsequently amplified with oYG726 and oYG727 using the initial PCR product as template. pDR183 is a double crossover integration vector at the *lacA* locus with an *erm* cassette (laboratory stock).

**pYG360[*yhdG::PxylA-spoVAF(phleo)(amp)*]** was constructed in a 2-way isothermal assembly reaction with a PCR product containing *spoVAF* amplified with oYG669 and oYG740 using gDNA of *B. subtilis 168*, and plasmid pCB109 cut with HindIII and XhoI. pCB109 is a double crossover integration vector at the *yhdG* locus with a *phleo* cassette and a xylose-inducible promoter P*xylA* (laboratory stock).

**pYG377[*yhdG::$P_{VA}$-spoVAF(V371L)(spec)(amp)*]** was constructed by site-directed mutagenesis using primers oYG750 and oYG751, and pYG07 as template.

**pYG378[*yhdG::$P_{VA}$-spoVAF(Q375L)(spec)(amp)*]** was constructed by site-directed mutagenesis using primers oYG752 and oYG753, and pYG07 as template.

**pYG386[*yhdG::$P_{VA}$-spoVAF(V371L)-gfp(spec)(amp)*]** was constructed by site-directed mutagenesis using primers oYG750 and oYG751, and pYG105 as template.

**pYG387[*yhdG::$P_{VA}$-spoVAF(Q375L)-gfp(spec)(amp)*]** was constructed by site-directed mutagenesis using primers oYG752 and oYG753, and pYG105 as template.

**pYG388[*yhdG::$P_{VA}$-spoVAF(V371L)-proC(spec)(amp)*]** was constructed by site-directed mutagenesis using primers oYG750 and oYG751, and pYG341 as template.

**pYG389[*yhdG::$P_{VA}$-spoVAF(Q375L)-proC(spec)(amp)*]** was constructed by site-directed mutagenesis using primers oYG752 and oYG753, and pYG341 as template.

**pYG415[*yvbJ::yqhR(kan)(amp)*]** was constructed in a 2-way isothermal assembly reaction with a PCR containing yqhR and its native promoter amplified with oYG551 and oYG799 using gDNA of *B. subtilis 168*, and plasmid pCB47 amplified with oYG292 and oYG293. pCB47 is a double crossover integration vector at *yvbJ* locus with a *kan* cassette.

**pYG416[*yvbJ::yqhR(Y146A)(kan)(amp)*]** was constructed by site-directed mutagenesis using primers oYG800 and oYG801, and pYG415 as template.

**pYG417[*yvbJ::yqhR(Y149A)(kan)(amp)*]** was constructed by site-directed mutagenesis using primers oYG802 and oYG803, and pYG415 as template.

**pYG432[*yvbJ::yqhR(Y146A)-His8(kan)(amp)*]** was constructed by site-directed mutagenesis using primers oYG800 and oYG801, and pYG238 as template.

**pYG433[*yvbJ::yqhR(Y149A)-His8(kan)(amp)*]** was constructed by site-directed mutagenesis using primers oYG802 and oYG803, and pYG238 as template.

**pYG540[*yhdG::PxylA-spoVAF-mYpet(phleo)(amp)*]** was constructed in a 2-way isothermal assembly reaction with a PCR product containing *mYpet* amplified with oYG738 and oYG739 using plasmid pWX318 (laboratory stock), and plasmid pYG360 amplified with oYG737 and oYG282.

**pYG546[*yhdG::Phy-spoVAF-proC(erm)(amp)*]** was constructed in a 2-way isothermal assembly reaction with a PCR product containing *spoVAF-proC* amplified with oYG608 and oYG618 using pYG318, and pCB100 cut with HindIII and SpeI. pCB100 is a double crossover integration vector at the *yhdG* locus with an *erm* cassette and IPTG-inducible promoter Phyperspank (laboratory stock).

**pYG563[*yhdG::$P_{VA}$-spoVAF-FLAG(spec)(amp)*]** was constructed in a 2-way isothermal assembly reaction with a PCR product amplified with oYG75 and oYG1048 using pYG351, and pCB179 amplified with oYG74 and oYG109. pCB179 is a double crossover integration vector at *yhdG* locus with a *spec* cassette and the promoter of *spoVA* operon ($P_{VA}$).

All plasmids were confirmed by Sanger sequencing.

**SUPPLEMENTAL REFERENCES**


1. Gao Y, Amon JD, Artzi L, Ramirez-Guadiana FH, Brock KP, Cofsky JC, et al. Bacterial spore germination receptors are nutrient-gated ion channels. Science. 2023;380(6643):387-91. Epub 20230427. doi: 10.1126/science.adg9829. PubMed PMID: 37104613.
2. Zeigler DR, Pragai Z, Rodriguez S, Chevreux B, Muffler A, Albert T, et al. The origins of 168, W23, and other Bacillus subtilis legacy strains. J Bacteriol. 2008;190(21):6983-95. Epub 20080822. doi: 10.1128/JB.00722-08. PubMed PMID: 18723616; PubMed Central PMCID: PMCPMC2580678.
3. Gao Y, Barajas-Ornelas RDC, Amon JD, Ramirez-Guadiana FH, Alon A, Brock KP, et al. The SpoVA membrane complex is required for dipicolinic acid import during sporulation and export during germination. Genes Dev. 2022;36(9-10):634-46. Epub 20220602. doi: 10.1101/gad.349488.122. PubMed PMID: 35654455; PubMed Central PMCID: PMCPMC9186386.
4. Taguchi A, Welsh MA, Marmont LS, Lee W, Sjodt M, Kruse AC, et al. FtsW is a peptidoglycan polymerase that is functional only in complex with its cognate penicillin-binding protein. Nat Microbiol. 2019;4(4):587-94. Epub 20190128. doi: 10.1038/s41564-018-0345-x. PubMed PMID: 30692671; PubMed Central PMCID: PMCPMC6430707.